The Thesis committee for Tai Anh Duong

Certifies that this is the approved version of the following thesis:

Heat Waste Recovery System from Exhaust Gas of Diesel Engine to a Reciprocal Steam Engine

APPROVED BY

SUPERVISING COMMITTEE:

Supervisor:_____

Ronald Douglas Matthews

_____

Matthew John Hall

Heat Waste Recovery System from Exhaust Gas of Diesel Engine to a Reciprocal Steam Engine

by

Tai Anh Duong, B.S.

Thesis

Presented to the Faculty of the Graduate School

of the University of Texas at Austin

in Partial Fulfillment

of the Requirements

for the Degree of

Master of Science in Engineering

The University of Texas at Austin

August 2011

Dedicated to my parents and the members of Taos: Bian Tagal, Kent Lau, Alex Ko, Tommy Cai, Marwan Harajli... who made this thesis possible.

Acknowledgements:

Many faculty and students helped made this study possible, namely Dr. Matthew John Hall for his guidance in the Yanmar diesel engine, Demintry in helping with steam engine. I would like to extend my appreciation to Tho Huynh for his helpful guidance and equipment in electronic circuits. I also want to thank Mark Phillips for his knowledge in injector fuel and electronic advice. And most importantly, Dr. Ronald Douglas Matthews for guidance and direction on completing this groundbreaking work.

Heat Waste Recovery System from Exhaust Gas of Diesel Engine to a Reciprocal Steam Engine

by

Tai Anh Duong, M.S.E.

The University of Texas at Austin, 2011

Supervisor: Ronald Douglas Matthews

Abstract

This research project was about the combined organic Rankine cycle which extracted energy from the exhaust gas of a diesel engine. There was a study about significant properties of suitable working fluids. The chosen working fluid, R134a, was used to operate at the dry condition when it exited the steam piston engine. Furthermore, R134a is environmentally friendly with low environmental impact. It was also compatible with sealing materials. There were calibrations for the components of the combined Rankine cycle. The efficiency of the heat exchanger converting exhaust heat from the diesel engine to vaporize R134a was 89%. The average efficiency of the generator was 50%. The hydraulic pump used for the combined Rankine cycle showed a transporting problem, as vapor-lock occurred when the pump ran for about 1 minute. The output of the combined Rankine cycle was normalized to compensate for the parasitic losses of a virtual vane pump used in hydraulic systems for the 6 liter diesel engines. There were three different vane pump widths from different pumps to compare frictional loss. The pump with the smallest vane width presented the least frictional mean effective pressure (0.26 kPa) when scaled with the displacement of the GMC Sierra 6 liter diesel engine. The power output of the Rankine cycle was scaled to brake mean effective pressure to compare with the frictional mean effective pressure. The maximum bmep was at 0.071 kPa when diesel engine had rotational speed at 2190 RPM. The power outputs

of the organic Rankine compensated partially the frictional loss of the vane pumps in the 6 liter diesel engine. By using R134a, the condensing pressure was 0.8 MPa; hence, the power outputs from steam engine were limited. Therefore, refrigerants with lower condensing pressure were needed. There were proposal for improvement of the organic Rankine by substituting R134a by R123 (0.1 MPa), R21 (0.2 MPa), and R114 (0.25 MPa) .

Contents:

List of Tables

List of Figures

1 Introduction

Recently, the National Highway Traffic Safety Administration, the division of the United State Department of Energy that is responsible for fuel economy standards, made two important announcements. One of these announcements was that Corporate Average Fuel Economy Standads will become much more stringent- increasing from 27.5 mpg (1990-2010) to 54.5 mpg in 2025. The other announcement was that heavy duty vehicles will finally become subjected to fuel economy standards- with separate standards for the engine and for the vehicle. Thus, after fuel efficiency standards were stagnant for two decades, methods for improving fuel economy have become of urgent interest. One method that is already being pursued is hybridization. Another method is to utilize the "waste heat" from the engine.

In this research project, I evaluated the performance of an organic Rankine cycle coupled with a diesel engine. The waste heat from the diesel engine would be used as the heat source to provide energy to a Rankine cycle engine that uses an organic working fluid. First, I analyzed the amount of heat waste from the diesel engine to the current setup. Then I evaluated the thermoenergy heat transfer to the refrigerant, I could also evaluated the efficiency of the heat exchanger. I explored many safety and environmental impact properties of the refrigerant, as well as the compatibility with materials in the organic Rankine cycle. I observed the generator measuring the power output of the Rankine cycle. Finally, we will calculate the brake mean effective pressure of the Rankine cycle compared to the frictional mean effective pressure of parasitic loss of vane pumps used on a GMC Sierra 6 liter diesel engine.

Chapter 2 showed the review of previous literature about organic Rankine cycle utilized waste heat with temperature below 500^oC. This chapter also presented thermodynamic properties and safety data of refrigerants. This chapter was the guidance to choose the appropriate refrigerant for my organic Rankine cycle. It also presented several other methods utilized waste heat at low temperature.

Chapter 3 demonstrated the organic Rankine cycle setup. This chapter showed details

of all the components in the cycle. It also illustrated a calibration setup for generator, a pressure adjustment setup for the pump.

Chapter 4 presented the result of all the experiments. The first portion of this chapter presented the result and linear curve fit of the dynamometer for the diesel engine to determine the torque. This chapter also presented the efficiency of the generator used in the organic Rankine cycle. Next, this chapter showed the potential waste recovery from the diesel engine from the heat transfer rate in the heat exchanger. This chapter exhibited the thermodynamic energy provided to the steam engine, and its efficiency. This chapter presented the entire thermodynamics properties condition of refrigerant in the organic Rankine cycle. From the power output, I evaluated the energy per unit mass of diesel fuel used in this research project. There was also an introduction of virtual loss from frictional loss of several vane pump models used in hydraulic system in a GMC Sierra 3500 diesel engine. These virtual frictional loss were scaled to frictional mean effective pressure (fmep). The power output of the organic Rankine cycle were scaled as brake mean effective pressure (bmep) to compensate for the frictional loss from the vane pumps.

Chapter 5 presented the conclusions of all the results. This chapter presents the limitation of components in the system which led to the inefficiency of the the organic Rankine cycle. This chapter also offered some of the recommendations to improve the efficiency of the organic Rankine cycle.

2 Review of Previous Work:

There are many industrial processes which continuously reject heat below 500^oC into the environment. This exhaust heat is generally considered as waste and dumped into the atmosphere and/or a water reservoir. With new regulations by the Environment Protection Agency (EPA), industrial plants must now limit their thermal discharge to the environment. This stringent regulation is the driving force for plants to find solution for the thermal load or better recycle this heat to usable energy. In light of those regulations, new facilities are being built and new methods are being implemented to utilize and recycle waste heat into useful energy.

Our concentration is about recycling the waste heat from diesel engines to power the reciprocal expander in an organic Rankine cycle. This chapter focuses on the Rankine cycle and its derivative which is the organic Rankine cycle, the Diesel engine cycle, the choice of working fluid, and other solutions for low temperature heat recovery.

2.1 The Rankine Cycle:

A Rankine cycle is a model of the steam-operated heat engine found in many power generation plants. Most of the combustion processes of coal, natural gas, oil, and nuclear fission reactions generate energy for the Rankine cycle. The working fluid is an important factor to the efficiency of the Rankine cycle. It is crucial to obtain the critical pressure of working fluid to optimize the efficiency of the Rankine cycle by increasing the temperature difference across the cycle. The working fluid in a Rankine cycle follows a closed loop and is circulated constantly. There are many substances that can be used as working fluid in the Rankine cycle; water is usually the fluid of choice due to its non-toxicity, non-flammability, and low cost. The main advantage of the Rankine cycle is using a pump to increase the pressure. The pump does not require much energy compared to the energy generated from the expander or turbine [6].

The four fundmental processes in the Rankine cycle are compression, evaporation (heat addition), expansion, and condensation (heat rejection). Process 1-2 is the liquid

compression; the working fluid is pumped from low pressure to high pressure. The working fluid is in liquid state, hence it requires a nominal amount of energy to pump.

$$w_p = -\int_1^2 v dP = v_l(P_1 - P_2) \quad (1)$$

where v_l is the specific volume of the saturated liquid working fluid.

Process 2-3 is evaporation. This is an isobaric process; liquid is heated in the boiler at constant pressure to saturated or superheat vapor at the outlet. The Mollier diagram or P-h diagram, illustrates the energy input to the system.

Process 3-4 is expansion in the expander or turbine. The vapor expands through a turbine and generates power. The pressure, temperature, and quality of the working fluid all decrease during this ideally isentropic process. The Mollier chart provides the enthalpy data to calculate the energy output in this process. Finally, process 4-1 is condensation. The wet vapor enters a condenser to condense back to liquid state at a constant pressure.

The organic Rankine cycle uses different organic working fluids such as R-134a or R-123 instead of conventional water. The exhaust gas which is about $300 - 500^oC$ will vaporize the organic working fluids from the waste heat from diesel engine at full load, . However, the difference between the maximum and minimum temperature of the working fluid is not high, hence the efficiency of the system is relatively low compared to the Rankine cycle that is not using low temperature waste heat as the heat sources. On the other hand, the system setup is simple and easy to retrofit into an automobile engines. This is also one of the motivations for this project. The organic Rankine cycle is more appropriate for the low temperature input system. The Rankine cycle does not constitute a specific working fluid in its definition, so normal Rankine cycle thermodynamics can be applied to different working fluids. However, choosing the right working fluid depends on many other factors which are elaborated in the next sections.

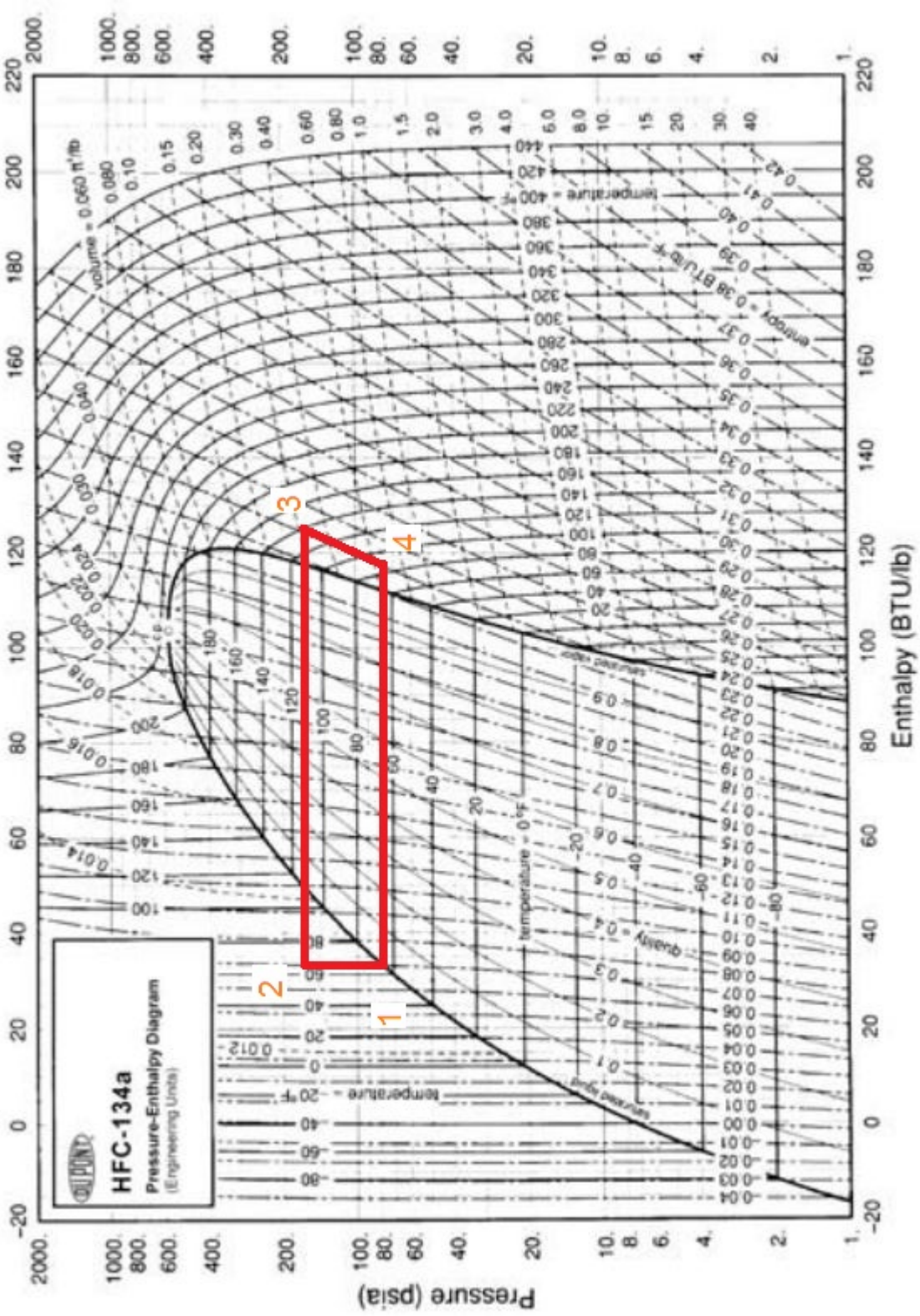

Figure 1: Mollier Diagram

2.2 The Diesel Engine Cycle:

For this project, a 10-HP diesel engine was used to supply waste heat into the working fluid for a steam engine. The diesel engine is widely used because it has a higher efficiency than a gasoline engine . The exhaust of the diesel engine is process 4-1 and 1-2 in Figure 2.

I wanted to estimate the ideal of amount of waste heat from the diesel engine. At one specific ideal operating condition, this Yanmar 100AE diesel engine provides 7.7 HP or 5.8 kW at 2500 RPM. In one hour, the work output of the diesel engine is 20.79 MJ. Based on the data provided from the manufacturer [1], the energy density of diesel fuel is $41.76\,MJ/kg$ [9] at 2500 RPM. Specific fuel consumption for a diesel engine at this speed is 48.9 g/MJ.

Fuel consumption for one hour is:

$$Fuel \quad = \quad \frac{specific\,fuel\,cons. \times energy\,output}{1000} = \frac{20.79 \cdot 48.9}{1000} = 1.01\,(kg/h) \qquad (2)$$

The energy output for this amount of fuel is:

$$Energy \quad = \quad fuel \times energy\,density = 1.01 \times 41.76 = 42.51\,(MJ/h) \qquad (3)$$

The ideal efficiency of diesel engine at 2500 RPM is:

$$\eta \quad = \quad \frac{energy\,output}{energy\,input} \times 100\% = \frac{20.79}{42.51} = 49\% \qquad (4)$$

The waste heat from the diesel engine at 2500 RPM is:

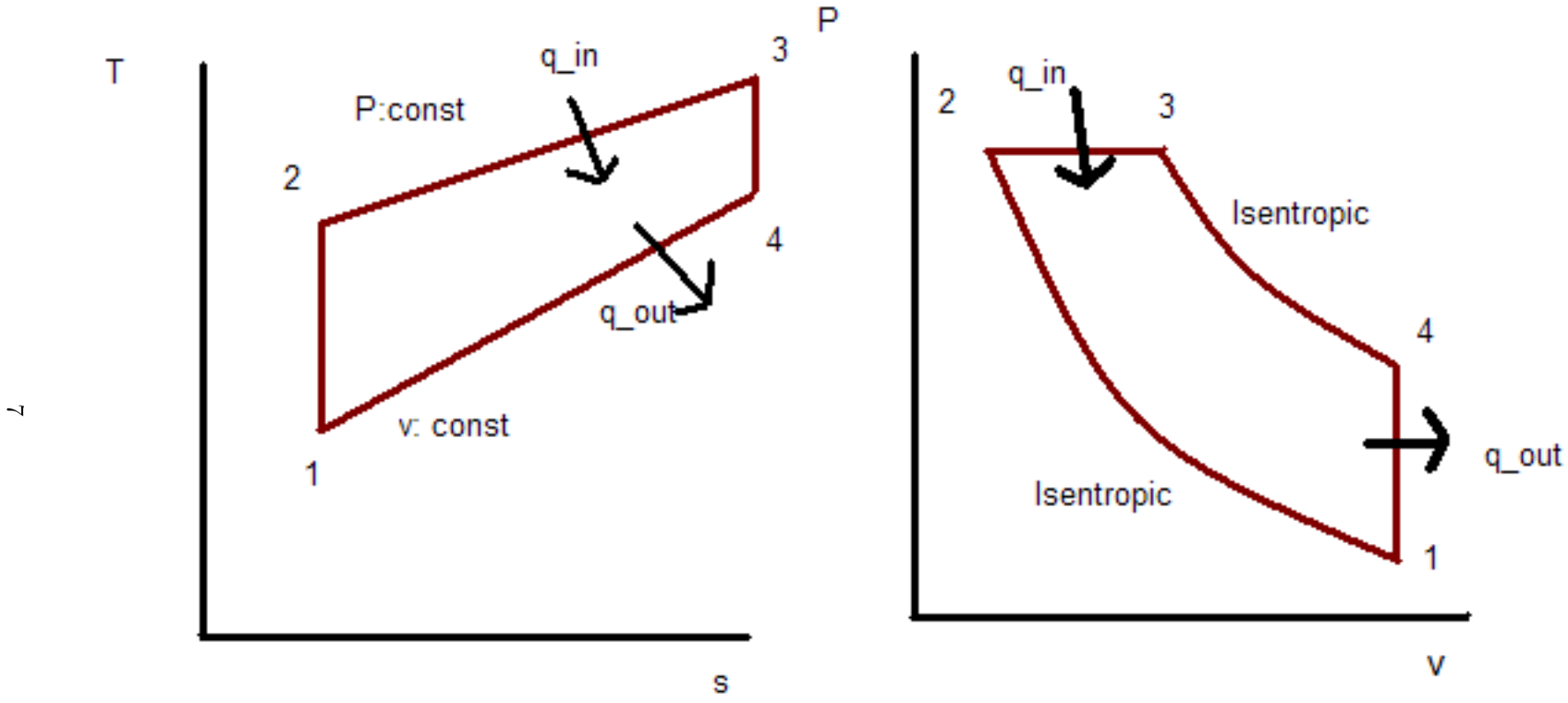

a) b)

Figure 2: T-s and P-v diagram of Ideal Diesel Cycle

$$waste\,heat \quad = \quad 42.51 - 20.79 = 21.72\,(MJ) \tag{5}$$

With the same method of calculation, the efficiency of diesel engine operating at 3600 RPM is $\eta = 31.3\%$ and consumes 2.05 kg diesel fuel.

Since this diesel engine waste heat is the heat source, it is crucial to compute the exhaust heat from the engine to our organic Rankine cycle. At 2500 RPM operation, the heat rejected to our system is 21.71 MJ for each hour. Hence, it is profitable to exploit the waste heats and recover it in the organic Rankine cycle.

2.3 Choice of working fluid:

It is critical to choose a proper working fluid in an organic Rankine cycle. Since the heat source from the exhaust of a diesel engine at low temperature, the thermodynamic properties of the working fluid significantly impact the performance of the system. The main purpose of an organic Rankine cycle is to extract heat from the low temperature heat power from the exhaust gas of a diesel engine. However, the manufacturer stated the upper limit of steam engine is about 250 psi, therefore, the critical condition of R134a cannot be obtained.

Figure 3 shows the saturation vapor curve in the T-s diagram can have positive, negative or vertical slope.

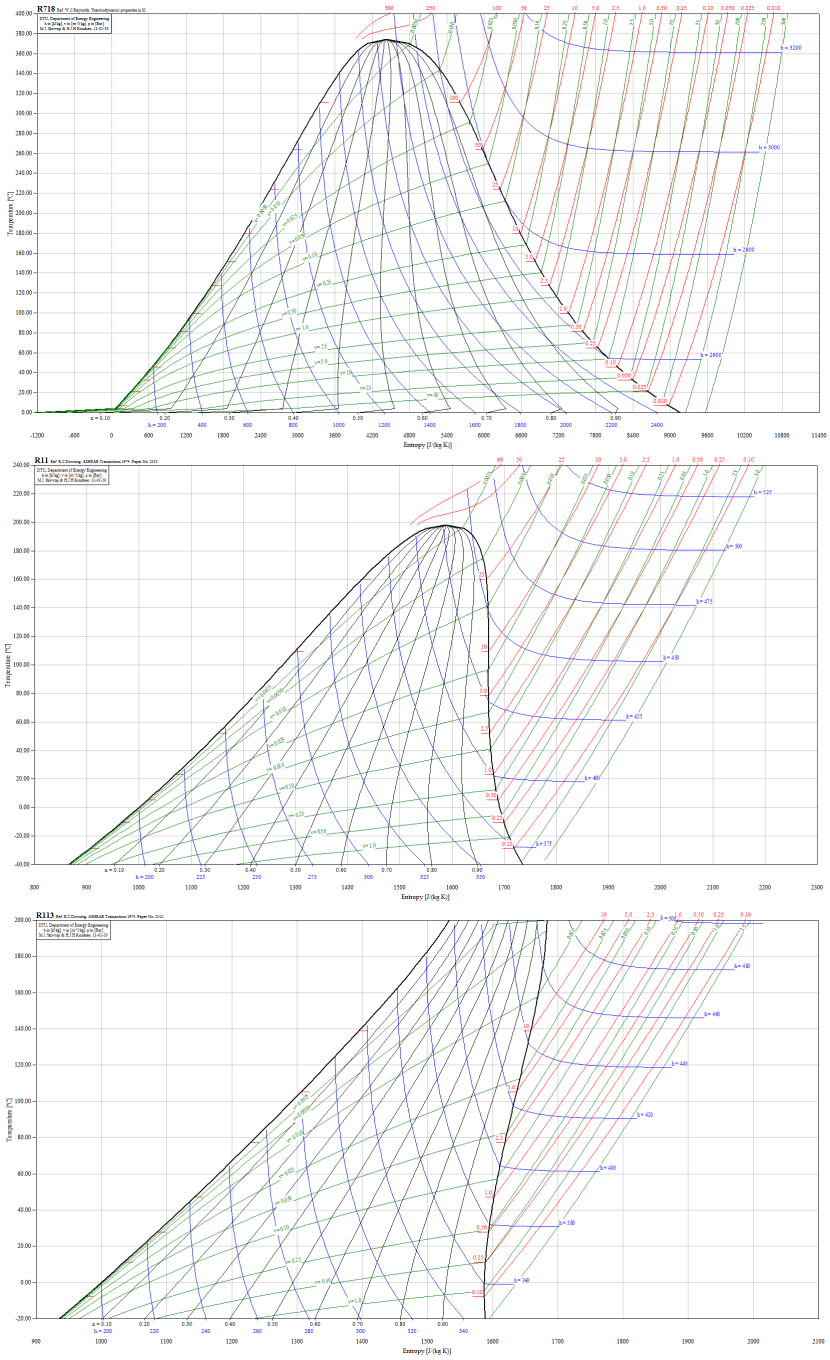

Figure 3: Negative (water curve), isentropic(R-11 curve), and positive(R-113 curve) slope saturation vapor curve. The curves are obtained from COOLPACK

In the expansion process, it is undesirable to have condensation inside the steam engine. Hence we would like to choose a working fluid that has the saturation curve parallel to the isentropic expansion in the Rankine cycle. For the wet working fluids, the slope of the vapor curve is downward or negative. Therefore, the isentropic expansion curve will end up with condensing inside the expander. The condensation might corrode the cylinder in the long run. For "dry" working fluids, the slope of the saturated vapor curve is upward or positive. In this case, at the exit point of the expander, the working fluid is still vapor. The optimum characteristic for Rankine cycles is a positive saturation vapor curve like R 113. However, it is illegal to purchase this type of refrigerant without handling permit. In our research project, the R134a has a wet vapor curve slope; therefore, the refrigerant was heated to the condition that ensures the refrigerant at the outlet of the steam engine still in vapor state.

Safety codes may require a non-flammable refrigerant of low level of toxicity for our applications. Cost, availability, efficiency, and compatibility with our lubricants and materials with which the equipment, piping, and fittings are constructed are the main concerns.

Low freezing point, high stability temperature:

In contrast to water, many organic fluids cannot sustain the same composition at high temperature; they can be broken down into different chemicals. Therefore, it is critical to choose a working fluid that has the stability temperature higher than the maximum temperature of the exhaust gas. On the other hand, the working fluid might freeze, so the lowest temperature in the system needs to be higher than the freezing point. Therefore, it is crucial to select a working fluid which does not clog the system by freezing.

Low environment impact:

Fully halogenated compounds such as chloroflorocarbons (CFC) have persisted in the atmosphere for many years. However, when a refrigerant eventually leaks, it diffuses into

the stratosphere. Once in the upper atmosphere, CFC molecules chemically break down and release chlorine, which destroys ozone. This is known as Ozone Depleting Potential (ODP). In the lower atmosphere these molecules absorb infrared radiation, which may contribute to the warming of the earth. This is called as Greenhouse Warming Potential (GWP). By substituting a hydrogen atom for one or more of the halogens in a CFC molecule, it will greatly reduce its atmospheric lifetime and lessen its environmental impact. In our system, with much effort to eliminate leaking, the working fluid was sealed in the circuitry except at the piston rod of the steam engine. The manufacturer tried to seal the clearance at the piston rod, however, when the steam engine operates, there is vapor leaking from the steam engine cylinder.

Phase out of Refrigerants:

The Montreal Protocol is an international effort to regulate the production of ozone depleting substances, including refrigerants containing chlorine and/or bromine (U.N. 1994 and 1996). The Copenhagen Amendment called for a complete stop of the production of CFCs by Jan 1, 1996 [2]. However, continued use from existing stock is still permitted. HCFCs (like R-22 and R-123) are to be phased out relative to a 1989 reference level for developed countries. Production was frozen at the 35% reference level by January 1, 2010 to 10 % by Jan 1, 2015 and to 0.5 % of the reference level by Jan 1, 2020 [2]. The production and use of hydrofluorocarbon (HFC) refrigerants (such as R-32, R-125, R134a, R-143 and their mixtures, including R401A, R407C, and R401A) are not affected by the Montreal Protocol. Our choice of R-134a is still available in the market to purchase at the time of experiment. Other refrigerants, other than R134a, require customers to have refrigerant handling permits in order to purchase.

Safety is another concern. The refrigerant should not be toxic or flammable. ASHRAE Standard 34 [2] presents the safety classification via a capital letter and a numeral. The toxicity and flammability classifications yield six safety groups (A1, A2, A3, B1, B2, and B3). The capital letter denotes the toxicity of refrigerant at concentration below

$400\,ml/m^3$. Class A notifies the toxicity is not identified; while class B shows there is evidence of toxicity. The numeral warns about the flammability of the refrigerant. Class 1 indicates no flame propagation in the environment at room temperature 18^oC and $101\,kPa$. Class 2 exhibits lower flammability limit (LFL) greater than $0.1\,kg/m^3$ at 21^oC and $101\,kPa$ and heat of combustion less than $19000\,kJ/kg$. Class 3 denotes high flammability and capable to inflame lower or equal to $0.1\,kg/m^3$ at 21^oC and $101kPa$ or heat of combustion greater than or equal to $19\,000\,kJ/kg$.

When constructing the connections between the main components, the compatibility of refrigerant to materials should also be considered. Metal materials are used extensively throughout the system. Halogenated refrigerants can be used satisfactorily under normal conditions with most common metals, such as steel, cast iron, brass, copper, tin, and aluminum [2]. Under more critical conditions, hydrolysis and thermal decomposition are considered. Thermal decomposition of material is ranked in the following order: (least decomposition) $Inconel <\ 18-8\,stainless\,steel <\ nickel <\ copper <\ 1340\,steel <\ aluminum <\ bronze <\ brass <\ silver$(most decomposition). Magnesium, zinc, and aluminum alloys containing more than 2% magnesium should not be used with halogenated compounds where even a small amount of water is present.

Since the working fluid is circulated in a piping system at high pressure, sealing in the system is a crucial issue. In this system, several locations are sealed by O-rings. Refrigerants, lubricants, and mixtures of both can react with the elastomer to change its physical or chemical properties. Hamed[11] presented tables of compatibility of refrigerants, lubricants and elastomers. The weight change percentages after 14 days of formula #1 elastomer for R-22, R134a, and R123 are 43.9, 4.9, and 328 respectively. The similar patterns are repeated for different elastomers. Hence, caution should be taken to choose the refrigerant and O-rings.

Another important factor in the Rankine cycle is the lubricant. The list of lubricants and their miscibility is listed in Table 2. Polyol esters are used in HCFC refrigerant systems due to their physical properties [8]. Polyol ester is really stable in its thermal

Table 1: Working fluid characteristics

Working fluid	Slope of saturation/Vapor line [16]	Critical point	Safety [2]
water	wet	374 C- 220 bar	A1
R-11	Isentropic	198 C-44.1 bar	A1
R-22	Wet	96.1 C -49.9 bar	A1
R-113	Dry	214 C -34.4 bar	A1
R-123	Isentropic	184 C - 36.7 bar	B1
R-134a	Wet	101 C- 40.6 bar	A1
R-245fa	Isentropic	154 C- 36.4 bar	A1
R-601 (n-pentane)	Dry	196 C-33.6 bar	A3
R-601a (isopentane)	Dry	187 C -33.7 bar	A3
C6H6	Dry	289 C -49 bar	A3
C7H8 (Toluene)	Dry	319 C- 41 bar	A3
C8H10 (p-xylene)	Dry	343 C 35 bar	A3
HFO-1234	Wet	101.2 C 40.2 bar	A1
R507	Wet	70.3C 37.42 bar	A1
R-600 (Butane)	Dry	150C 37 bar	A3

Table 2: Lubricants for the working fluid R134a

Lubricant	Miscibility [15]	Cost ($/gallon)	
Mineral Oil	Non-miscible	29	
Alkyl Benzene	Non-miscible	62.9	
Polyol Ester	Miscible	117.6	

properties. The molecular structure of four carbons attached to one central carbon gives the thermal stability effect. Gunderson [10] performed a test with polyol esters and dibasic acid testers at 260^oC by heating them in evacuated tubes for up to 250 hours. He found that the compositions were not decomposed.

2.4 Other solutions for low grade heat recovery:

There are several other methods to recover energy from low grade heat source. Current developments with different advantages and drawbacks are discussed in the following subsections.

2.4.1 The water-ammonia cycle:

This cycle uses a mixture of water and ammonia as the working fluid. The mixture allows the temperature of the working fluid to increase during the boiling process. Hence this method improves the heat transfer process [13]. It turns out to have a better efficiency than the steam Rankine cycle in certain applications. However, its design is more complex than the Rankine cycles. Figure 4 represents the complexity of the ammonia-water cycles coupled with an internal combustion engine.

Jonsson [13] studied the energy output from two different systems of Rankine cycle bottoming, the spark-ignition gas engine and compression-ignition diesel engine. The exhaust gas from the two internal combustion engines provided the energy input to the water-ammonia cycles. The exhaust gas from the spark-ignition cycle is 100^oC higher than from the diesel engine. This study showed that when using diesel engines to provide energy input, the power for ammonia-water is lower than the spark-ignition

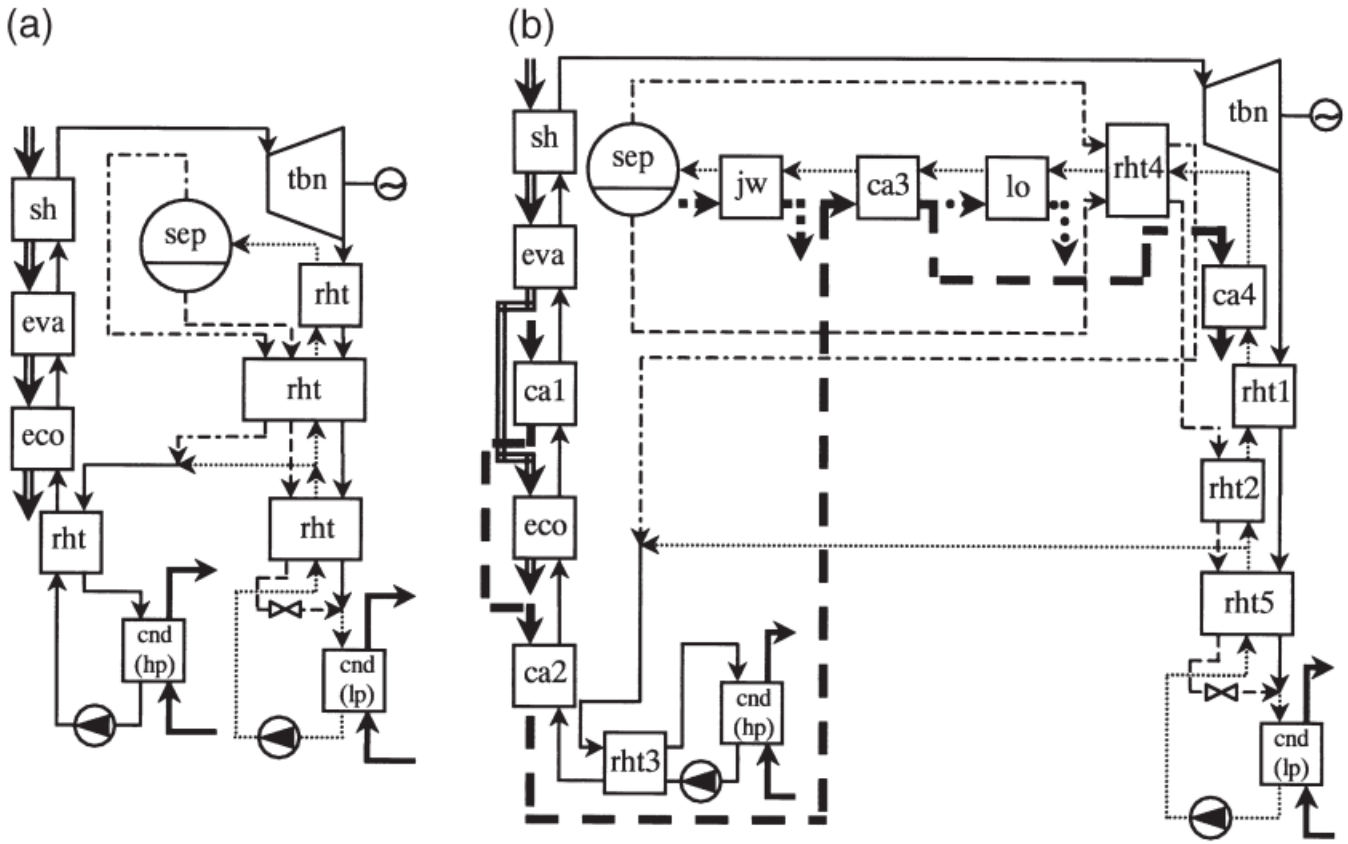

Figure 4: Ammonia-water system from Jonsson test bench with spark-ignition engine coupling is (a) and diesel engine coupling is (b)[13]

engine system. Figure 4 shows the schematic for water-ammonia cycle.

In Figure 4, the ammonia-water mixture goes through a non-isothermal phase change in the heat exchanger. It makes the temperature of the mixture attain higher temperature than a pure refrigerants from the waste heat. Therefore, in this process, the efficiency of combined water-ammonia is higher than Rankine cycle. However, there are a lot of components in these processes: reheat (rht), condensor (cnd), evaporation (eva), turbine(tbn), boiler(sh, eva, eco).

2.4.2 The Stirling and Ericssion cycle:

These cycles attain high theoretical efficiency [6]. The number of their practical applications is, however, limited since they require highly efficient heat transfer in the regenerator and at the heat source/sink level. The thermodynamic cycles of these two cycles are shown in Figure 5

2.4.3 Transcritical cycle:

Chen [7] reviews the carbon dioxide transcritical power cycle and the same system with R123. Since the waste heat which goes through the heat exchanger is a non-isothermal process, he used the mean temperatures as the reference temperature to compare the two systems. Carbon dioxide was heated beyond the critical condition [7]. The evaporation process is not in the vapor dome, hence the temperature increases through out the entire heat exchanger. The study concludes that the performance of the carbon dioxide transcritical system is higher than the one employing R123. This system is worth further study in the future because of the inert properties to the environment of carbon dioxide and the similar setup of the workbench. The thermodynamic cycle of the transcritical cycle is presented in Figure 6.

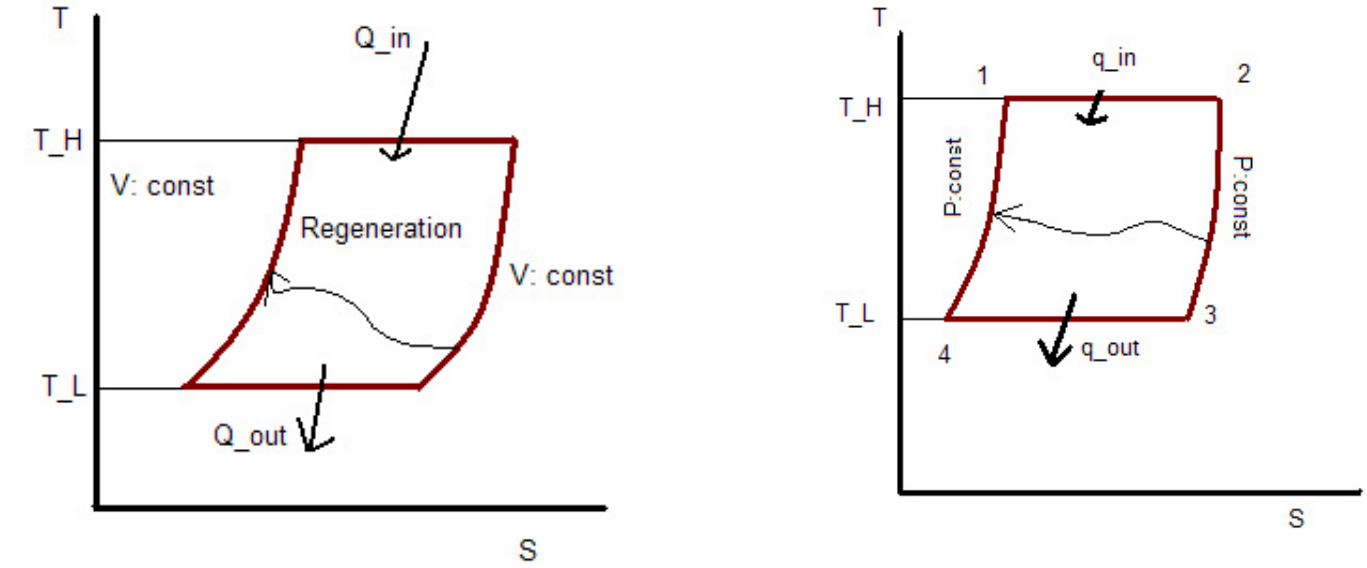

a) b)

Figure 5: T-s Diagram of Stirling cycles (a) and Ericsson cycles (b)

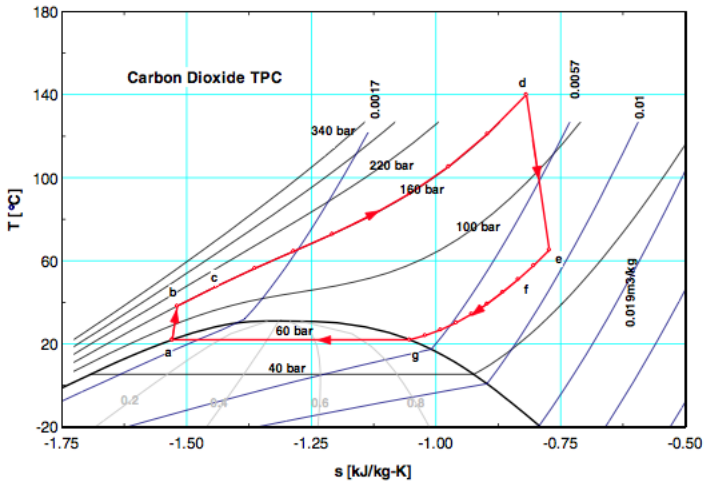

Figure 6: Thermodynamic cycle of transcritical cycle [7]

2.4.4 The Thermoelectric effect:

This method was first discovered by Thomas Seebeck. When two wires which are two different metals, are joined to form a closed circuit, and one of the junctions of this closed circuit is heated, a current flows continuously in the circuit. This phenomenon is applied in thermocouples. Since there are no mechanical moving parts, there is a huge potential for improvement in this process.

3 Description of the Organic Rankine Cycle Test Bench:

This section provides an overview of an experimental study carried out on a waste heat recovery Rankine Cycle test bench. In order to study the practicality of this cycle, a test bench was set up in the Engine Research Laboratory at the University of Texas at Austin. With this setup, one can evaluate the potential heat recovery efficiency from the heat exchanger, and determine the output work from the "steam" engine.

3.1 Configuration of the cycle:

As illustrated in Figure 7, a reciprocating pump transports working fluid inside the system. The pump only sustains a constant $1500\,psi$ pressure. Hence, an adjustable mechanism was installed after the pump to control the pressure of the working fluid before the working fluid enters the heat exchanger. Working fluid is heated in the evaporator to the saturation temperature corresponding to the pressure. The heat is provided by the exhaust gas from a diesel engine. A thermocouple, which is installed after the evaporator, sends the temperature reading to a multimeter to signal the moment to inject vapor into the reciprocating expander. With high temperature and high pressure, the working fluid will expand in the expander and produce power. Work is in the form of rotational torques and connects with a generator to produce electricity. The working fluid, after producing work, goes through the exhaust valve to condense back into liquid, then goes back to the pump.

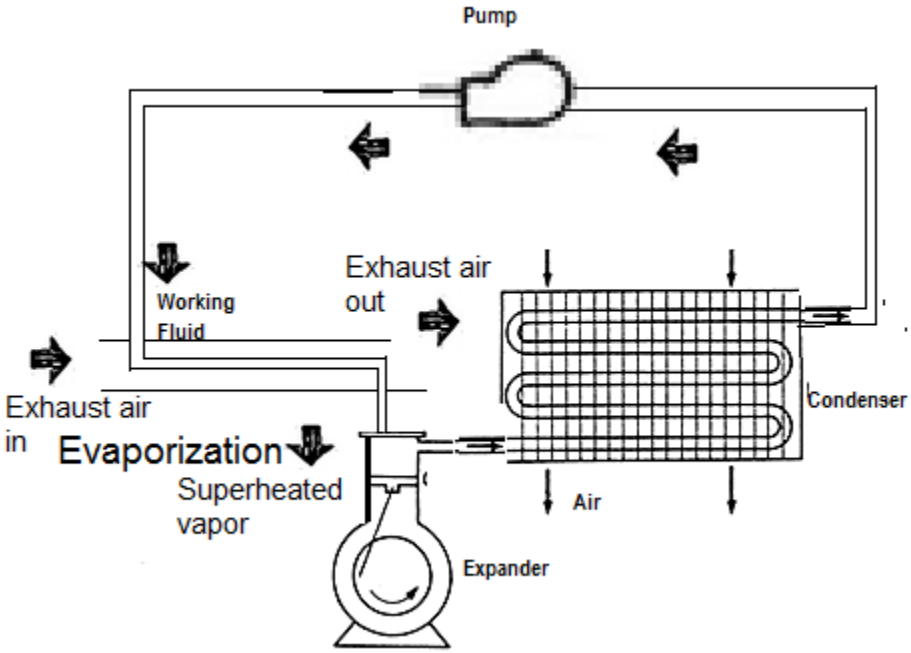

Figure 7: Flowing diagram for this setup

3.2 Reciprocating Expander:

The reciprocating expander is a double acting steam engine. The piston is connected to a crank mechanism which then turns a shaft. Experiments with pressures as low as 30 psi can provide a fair amount of torque[4]. This amount of torque produces electricity through a generator. Piston engines are easy to build, and due to their slow speed and general design, can last a very long time.

Figure 8 is the drawing of a typical steam engine cylinder components. In the current configuration, the slide valve opens up the back port allowing the steam to fill the cylinder on the backside of the piston. The valve will travel next to the rear of the cylinder, thereby uncovering the front port, and steam will rush in and push the piston back to the rear of the cylinder. At the same time, the center of the valve will uncover the rear cylinder port and allow the steam that was in the cylinder on the backside of the piston to exhaust out through the ports and into the exhaust chamber at the bottom of the

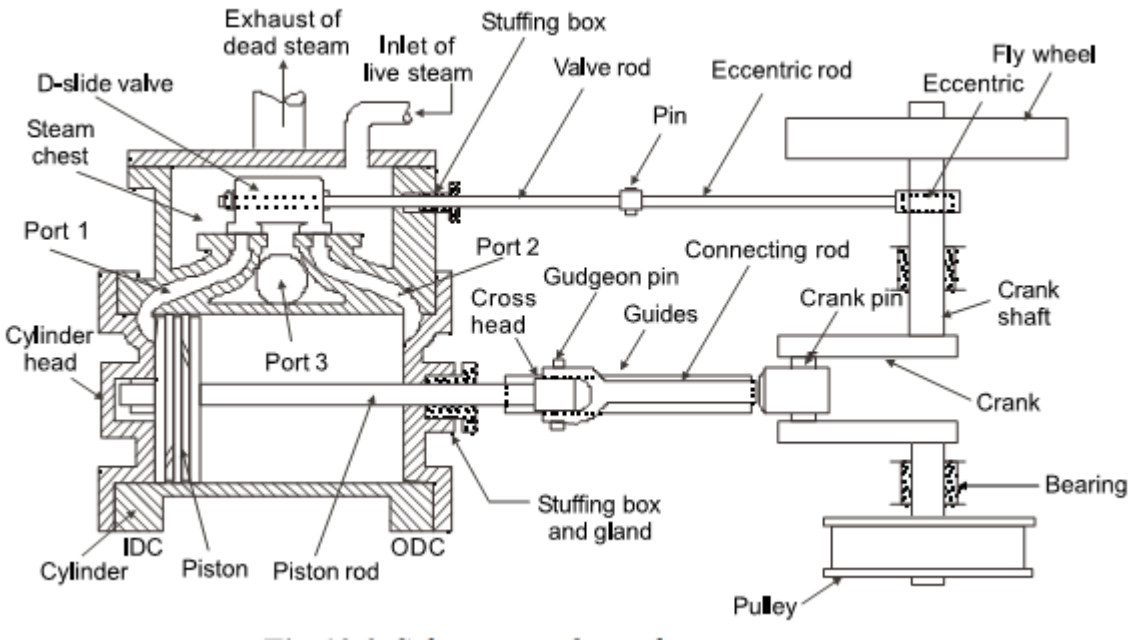

Figure 8: Steam cylinder components

D-slide valve. This action continues as the engine rotates and completes a full cycle for each revolution. Since steam is taken on both sides of the piston giving continuous power, this is known as a "double-acting" engine. Technically, this type of engine is of 'single stroke' design.

Figure 9 shows valve action in relation to the piston action. In the cylinder there are two ports connecting to the steam chest. These same ports will also allow steam to exhaust on through to the center exhaust port via a cavity on the bottom of the D-slide valve which is sealed off from the pressurized steam in the steam chest. In (A), we see the front port exposed to steam chest pressure which allows the steam to enter the cylinder and start to drive the piston back. At the same moment, the back port opens for the dead steam to exhaust through the exhaust cavity. In (B), we see the valve is now starting to travel forward and will soon cut off the steam admission from the front port and expose the rear port. The piston will continue on to the end of its stroke at the

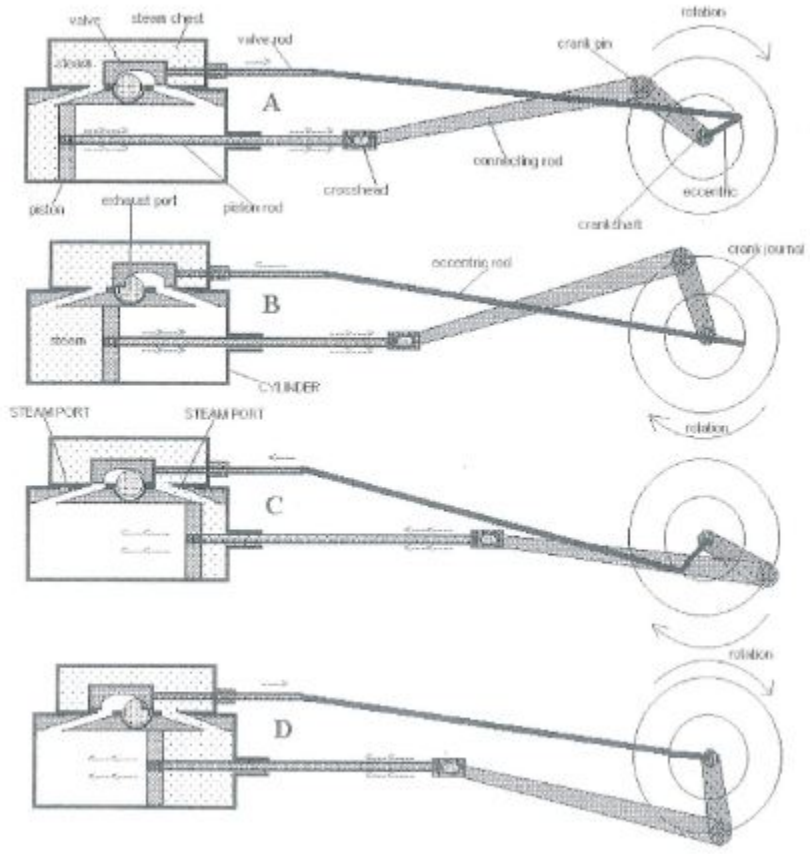

Figure 9: Motion and Timing of a double acting steam engine. Courtesy of Mike Brown[5]

rear of the cylinder. In (C), we now see how the valve has traveled forward, exposing the rear port to the pressurized steam and allowing that steam to enter the backside of the piston which will drive it forward. In (D), we see now the valve is started back in the original direction as the piston continues on forward. The valve will soon cover the rear port and expose the front port to begin the process all over again as shown in (A). It is important to study the timing of the eccentric; which drives the valve back and forth, in its relation to the crank journal; which is connected to the piston rod via the crosshead. Since steam is admitted on both sides of the piston, this type of steam engine is known as "double acting."

Basically, steam engines operate by admitting steam to one side of a piston. The other side of the piston is exposed to a much lower pressure. The low pressure side of the piston may be exposed to atmospheric pressure if the engine is known as "single acting."

A single acting engine only produces power for 50% of a revolution. This is a desirable condition where construction is meant to be inexpensive and/or light valve train is needed such as is common in high speed engines. Where maximum power is required in as small a power plant as possible, a steam engine may be designed to receive steam on both sides of the piston. This is known as a "double acting" engine. Both sides of the cylinder are sealed from the atmosphere and a valve system is used to admit and exhaust steam during alternate periods of the stroke. This is the type of engine seen in the Drawing 8. The entire action can be visualized in the series of drawings shown on Figure 9.

	Description
Type	double acting, single cylinder reciprocating
Material used	cast iron, aluminum, and stainless steel
Bore	1.5 "
Stroke	2.25"
RPM	600-700
Operating pressure	100 psi
Valve cutoff	55-70%
Valving	standard "D" valve with three cylinder ports
Rotation	clockwise

Table 3: Steam engine configuration

The cutoff ratio is represented as:

$$\Phi = \frac{v_5 - v_4}{v_6 - v_4} \tag{6}$$

where Φ is cutoff ratio, v_4 is the top dead center volume, v_5 is the admission volume, and v_6 is the bottom dead center volume. Based on the cutoff ratio, one can calculate the ideal power output of the steam engine.

3.2.1 Processes in the reciprocating expander:

The steam engine works on a modified Rankine cycle. The P-V diagram in Figure 10 presents the work output for steam engine versus clearance volume.

Live steam enters the cylinder at state 1' and steam injection continues up to state 2. Point 2 is showing the point at cut-off. Subsequently, steam is expanded up to state 3 theoretically and stroke gets completed. The expansion process is of hyperbolic type. A hyperbolic expansion process is one having the product of pressure and volume from 2-5 constant. In practice, the expansion process is not continued up to 3 due to the opening of the exhaust port. Hence, the expansion process is terminated even before this piston reaches the dead center. Figure 10 shows the thermodynamic cycle.

At state 5, the exhaust port is opened. Therefore, the pressure inside the cylinder drops just like the process from 5-6. The exhaust process happened from state 6 to 4. In our case, there was a clearance volume. So the exhaust process was modified to reflect this change.

Expansion ratio, $r = \frac{V_5}{V_2}$

The thermodynamics of the steam engine cycle with clearance volume cycle consideration work shall be:

$W = Area\, 1'2564'1'$

$W = Area\, 1290 + Area\, 2589 - Area\, 4680 - Area\, 11'4'4$

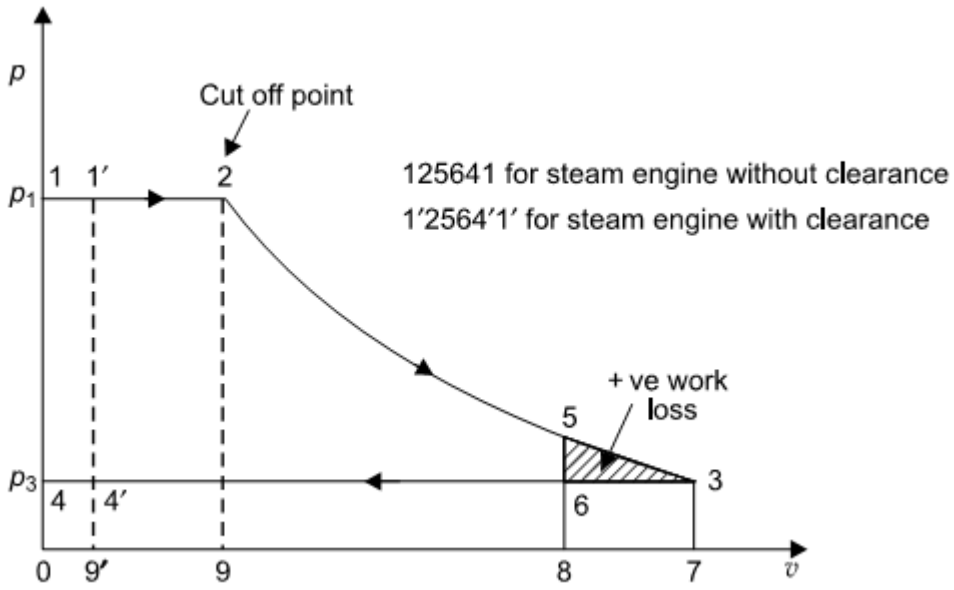

Figure 10: Modified Rankine cycle on P-V diagram for steam engines. [18]

$W = (p_1 V_2) + p_1 V_2 ln\left(\frac{V_5}{V_2}\right) - (p_3 V_6) - (p_1 - p_3)\, V_1'$

$W = (p_1 V_2) + p_1 V_2 ln\, r - (p_3 V_6) - (p_1 - p_6)\, V_1'$

and $V_5 = V_6$

3.2.2 Reason to choose a reciprocating expander:

There are two main types of expanders that can be used in an organic Rankine Cycle: turbomachines and the positive displacement type machines.Traditional power plants prefer to use turbomachines to generate electricity. For our purposes, the low-temperature heat recovery application, turbomachines present several challenges: The performance of turbomachines directly relates to the tip speed of the blade U(m/s), rather than shaft speed. There is a correlation between maximum performance and tip speed independent of machine size. A turbo-expander requires a high temperature load, otherwise, the efficiency of the turbomachine is low [16]. Further, the cost of a turbomachine is substantially higher than a reciprocating positive displacement expander.

Reciprocating positive displacement expanders are available off the shelf. It only requires direct connection to a steam engine.

3.3 Heat Source

The heat source used to supply input heat to the organic Rankine Cycle engine was a Yanmar L100AE Diesel engine (7.7-10 hp)

Figure 11: Yanmar L 100AE Diesel Engine

Continuous Rating Output	7.7 hp @ 3000 rpm
	9.0 hp @ 3600 rpm
Maximum Output	8.8 hp @ 3000 rpm
	10 hp @3600 rpm
Cylinders	1
Cooling System	Air
Bore ×stroke	$86 \times 70\,mm$
Displacement	0.406 litres
Dry Weight	48 kg
Length	417 mm
Width	470 mm
Height	494 mm

Table 4: Specification of Diesel Engine

The performance curve of the Diesel Engine used as the heat source for the Organic Rankine Cycle is presented in Figure 12. Based on the performance curve of the Diesel engine, the maximum power output is $10\,hp$ at $3600\,RPM$. For this experiment, the

shaft speed of the diesel engine was measured using a digital tachometer $DT2234C^{+}$.

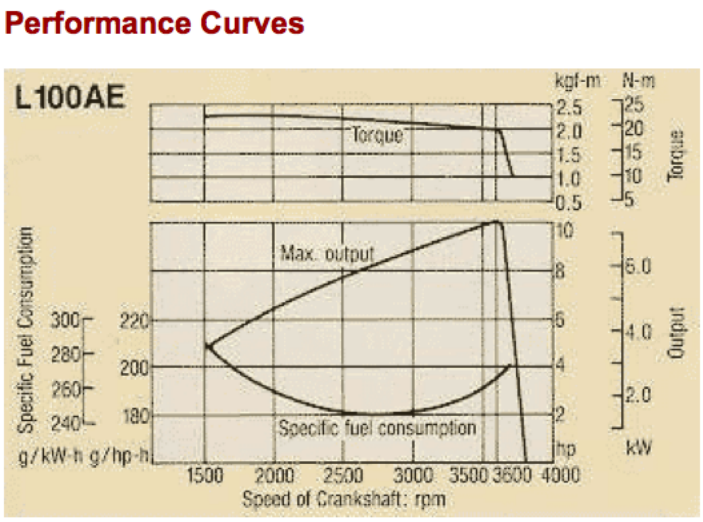

Figure 12: Performance Curve of Diesel Engine

Exhaust gas from the Diesel engine was coupled to a heat exchanger. Figure 13 shows a portion of the heat exchanger. The heat exchanger was a helical tube-in-tube counter flow heat exchanger. The outer tube contains the exhaust gas from the Diesel engine, while the inner tube transports the working fluid. The helical heat exchanger is designed to save space in the automobile applications. The helical motion creates more turbulence in the flow, which enhances heat transfer from waste heat to the Rankine cycle working fluid [14]. Along the tube length, there are baffles to create turbulence which will enhance heat transfer from the outer tube to the inner tube. Figure 13 shows the heat exchangers and its cross section.

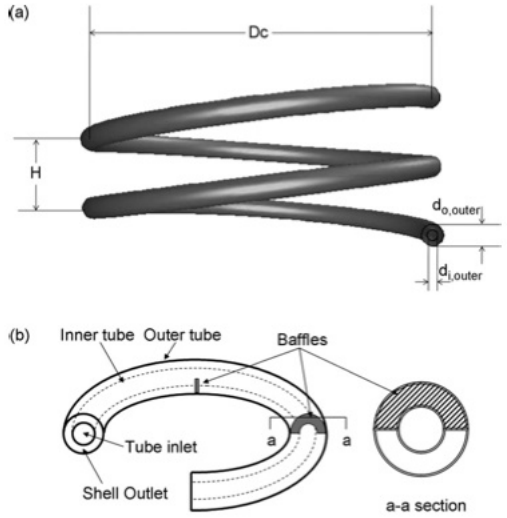

Figure 13: Heat exchanger

3.4 Generator

The electricity generator is a 1.5 horsepower permanent magnet generator(PMG)18. This PMG is constructed with a magnetic "rare earth" materials. The motor is used as a generator using input mechanical energy by coupling a chain to the shaft. However, there was no information about the performance of the generator. Hence, we put together a calibration set up for the generator. Figure 17 shows the calibration setup which includes two multimeters, a DC generator, a heater element, a 1 HP DC motor, a tachometer, and a constant 14 volt power supply.

The generator efficiency was determined by coupling the generator with a calibrated scooter motor. The free load speed and stall torque of the DC motor was determined to find the performance curve. Figure 14 shows the setup to characterize the performance of the the DC motor. In this setup, the tachometer is used to measure the free load speed of the DC motor. Then, torque is applied to the motor until stall condition is reached. The shaft of the motor is connect to a wrench as the moment arm. The length of the moment arm is 5.4 inches. The other side of the moment arm is connected to a

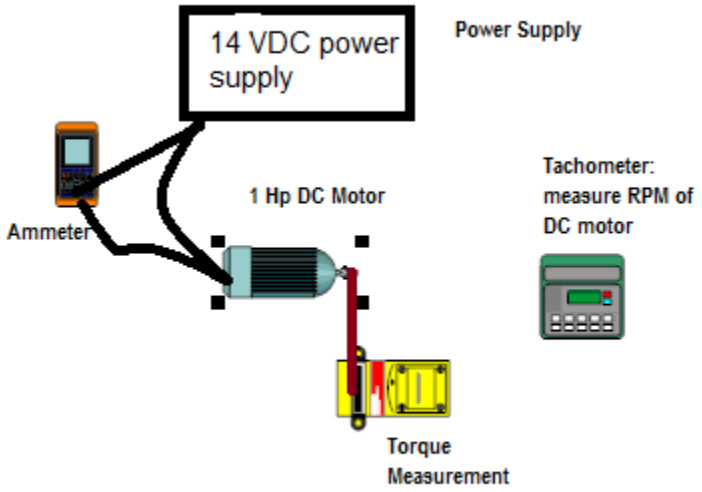

Figure 14: DC motor performance test setup

load cell to measure the force. The product of force and the moment arm length is the torque from the motor at stall condition. An ammeter is used to measured the power input to the motor. The performance of the DC motor is presented in figure. When the power input is 147 W, the free load speed is 570 RPM; the stall torque is 0.5 N-m.

The performance of the motor was evaluated in order to calibrate the generator. Figure 15 shows the power output of the motor versus the rotational velocity (rad/s).

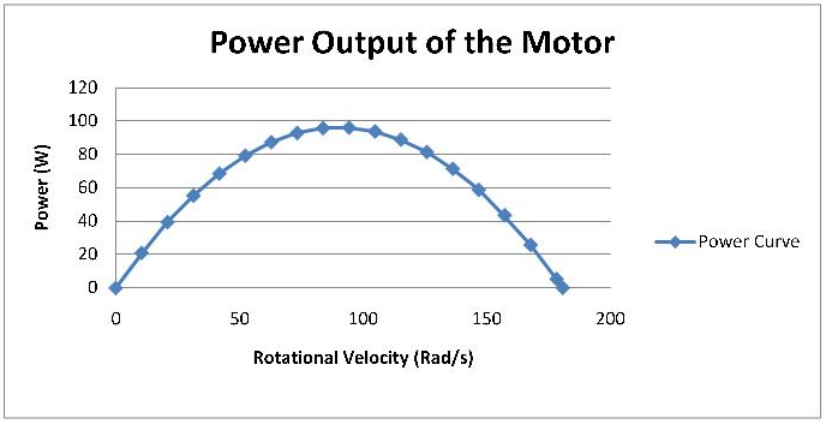

Figure 15: Characteristics of calibration motor

The results of the current input to the motor were presented in Figure 16. In this Figure, the current input decreased as the rotational speed of the motor increased. The behavior of current curve was the same as Micromon manual[17].

The information about torque and speed of the motor helps to find the efficiency of the generator. The generator is Permanent Magnet DC Treadmill Motor Wind Generator. Figure 17 shows the setup for the DC generator efficiency calibration. The same power supply provides energy to the DC motor. The DC motor is coupled with the DC generator. A tachometer is used to measured the RPM of the DC motor. From the performance curve of the DC motor, the torque is determined. Hence from the information about speed and torque, the mechanical power input into the DC generator is determined.

$$P_{mech} = T \cdot \omega \tag{7}$$

A heating element is used as the load for the DC generator. A multimeter is used to measure the voltage and current applied to the heating element. Therefore, the electrical power output of the DC generator is computed using the formula below.

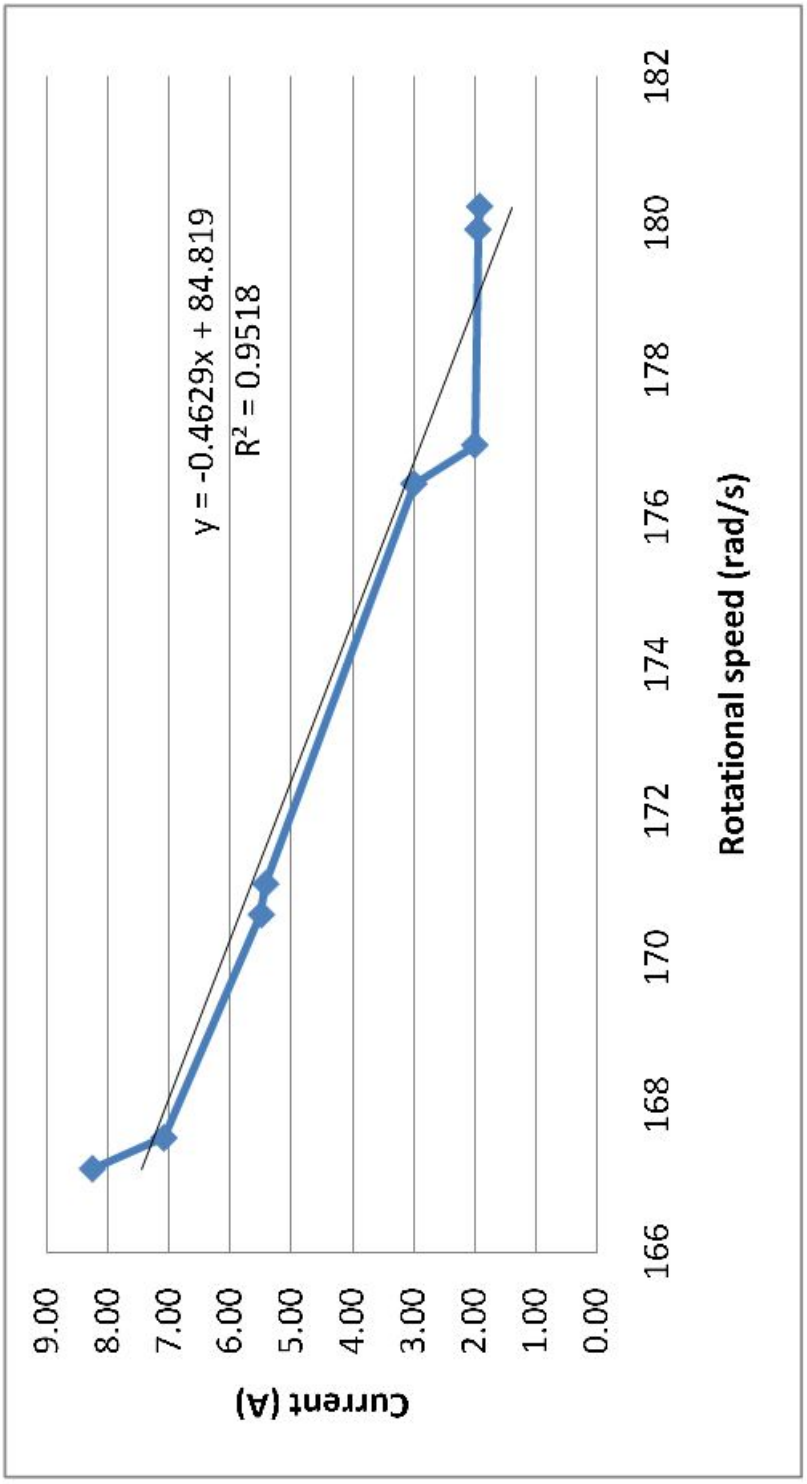

Figure 16: Input current to the motor

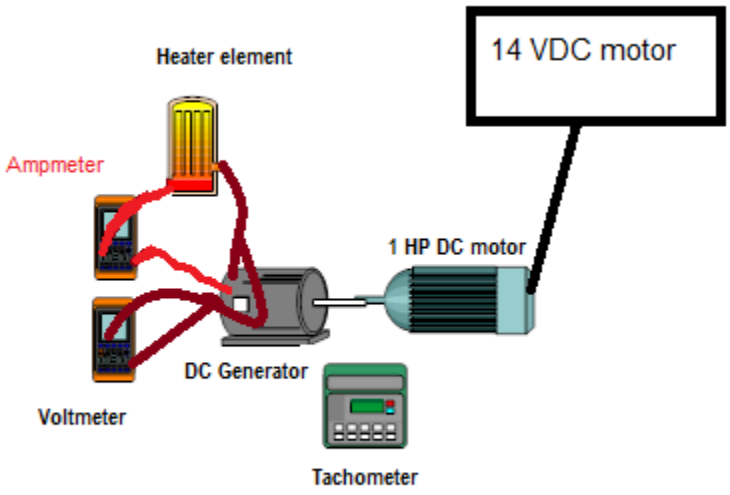

Figure 17: Setup for generator calibration

$$P_{electrical} = U \cdot I \tag{8}$$

The efficiency of the generator is calculated from the following equation:

$$\eta = \frac{P_{electrical}}{P_{mechanical}} \tag{9}$$

The result of calibration of the generator is shown in Result chapter. The description of the generator is detailed in Table 5.

Table 5: Specification of the 6.5 kW generator

Name	Permanent DC motor
Rotation	Clockwise
Voltage	100 VDC
Max RPM	5100
Max power	1.5
Main Usage	Treadmill

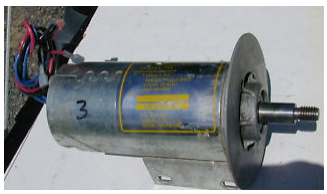

Figure 18: Permanent Magnet Generator

3.5 Pump

The pump is a hydraulic piston type pump (Figure 19). The pump draws fluid by a set of three pistons. The pressure from the pump can reach levels of 1500 psi. The pressure is controlled by a spring and switch mechanism. When the pump attains the specified pressure, the switch turns off the three pistons inside the pump.

Table 6: Technical Data of Husky Power Washer

Max rated pressure	1500 psi
Flow rate	1.4 gpm
Electrical requirement	120 V, 12.5 Amps, 60 Hz
Electrical cord	35 ft
High Pressure Hose	19 ft
Minimum Amperage source	15 amp
Pressure of inlet water	20-100 psi
Soap Consumption rate	6-10%
Inlet Water	Cold Tap Water

Figure 19: Husky power washer

The adjustable pressure mechanism is a simple setup composed of a needle valve and two pressure gauges. The needle valve reduces flow rate and pressure coming into the solenoid valve by branching out the flow back into the reservoir. From the reservoir, working fluid is circulated through the entire system.

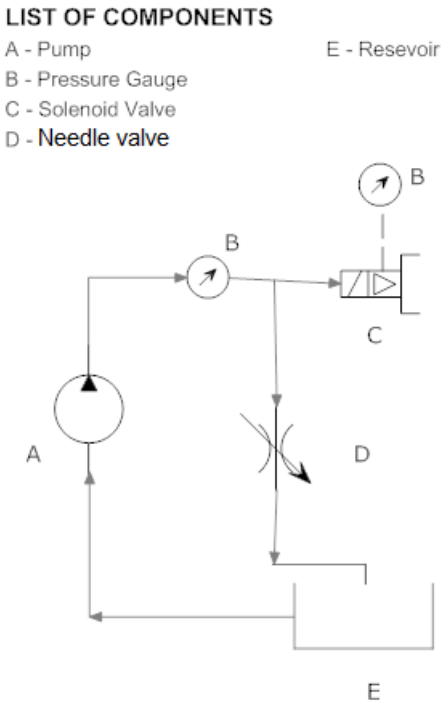

Figure 20: Adjustable pressure mechanism

4 Results of the Experiments

This chapter presented the results of the engine dynamometer for torque output, evaluation of the enthalpy flux in the engine exhaust gases for a given operating condition. The characterization of the electric motor and generator use to measure the power output of the Rankine cycle. Assessment of the efficiency of waste heat conversion to electricity and the net power output. The results were then used to model the performance of similar system were applied to a 6 liter displacement GMC Sierra 3500 diesel engine.

4.1 Characterization of Equipment

At first, the dynamometer coupled with the diesel engine was calibrated to determine the torque output of the engine when we adjust the air fuel ratio. The arm length of the dynamometer was 14 inches. Figure 21 shows the linear trend of the torque versus the voltage from the strain gage. This linear curve fit was used to measure the torque output of the diesel engine.

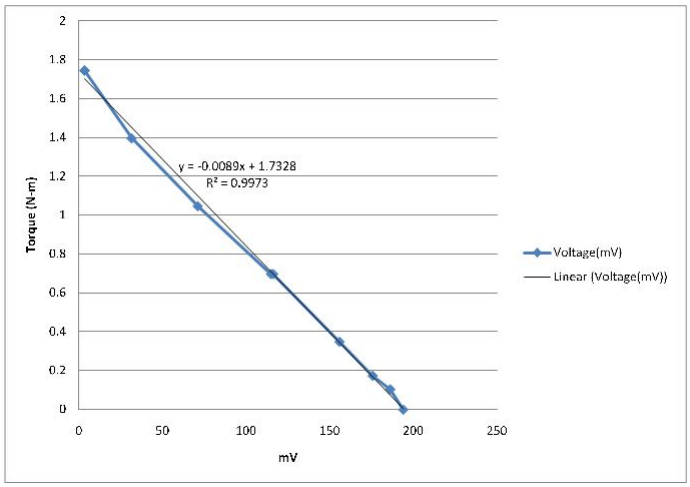

Figure 21: Calibration curve of the dynamometer used for the diesel engine

4.2 Evaluation of Amount of Waste Heat Recovery

I evaluated the performance and waste heat from the diesel engine provided to the organic Rankine cycle. After taking all measurements of waste heat through the heat exchanger and knowing the specification of the diesel engine, one can calculate the amount of waste heat. The cylinder displacement was 0.406 liter. When the diesel engine was operated, I used a tachometer to measure the rotational speed of the pulley connecting to the shaft of the diesel engine. From one evaluation of the waste heat of the diesel engine, the rotational speed of the shaft was 2273 RPM. Therefore, the flow rate of exhaust gas can be computed as:

$$Q = v\,(L) \cdot N\,(RPM)/(2 \cdot 60\,(s/min)) = 0.406 \cdot 2273/(2 \cdot 60) = 7.69\,(l/s) \quad (10)$$

Together with an air density of $1.23\,kg/m^3$, the mass flow rate is:

$$\dot{m} = Q\,(L/s) \cdot \rho\,(kg/m^3) \cdot 0.001\,(m^3/L) = 0.009\,(kg/s) \quad (11)$$

Temperature input and output of the exhaust gas through the heat exchanger were 500^oC and 80^oC . By using the average specific heat at 240^oC, which is 1.034 kJ/kg, one could calculate the heat transfer rate from the exhaust gas to the refrigerant (134a) :

$$q = \dot{m}\,(kg/s) \cdot c_p\,(J/kg) \cdot \Delta T\,(K) = 0.009 \cdot 1034 \cdot 420 = 4107\,(W) \quad (12)$$

Figure 22 shows the amount of waste heat recovery from the Diesel engine. As the rotational speed of the diesel engine increases, the exhaust gas mass flow rate increases. With constant temperature difference, the amount of waste heat increases as the rota-

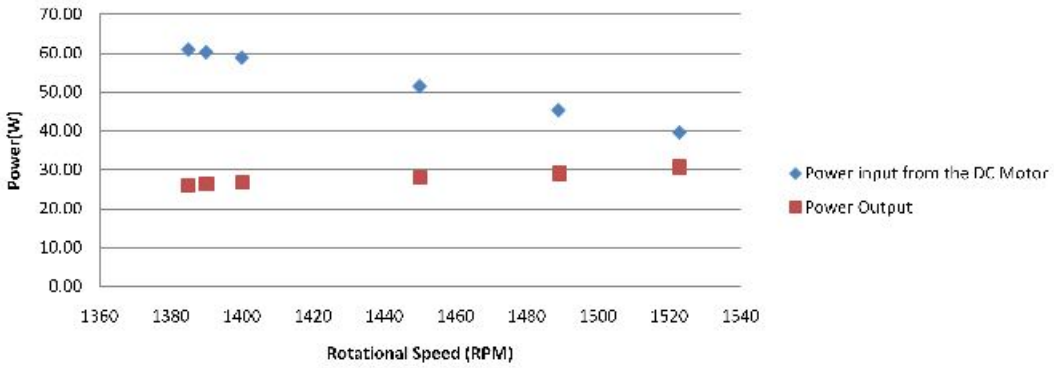

Figure 23: Performance of DC motor and generator

tional speed of the diesel engine increases.

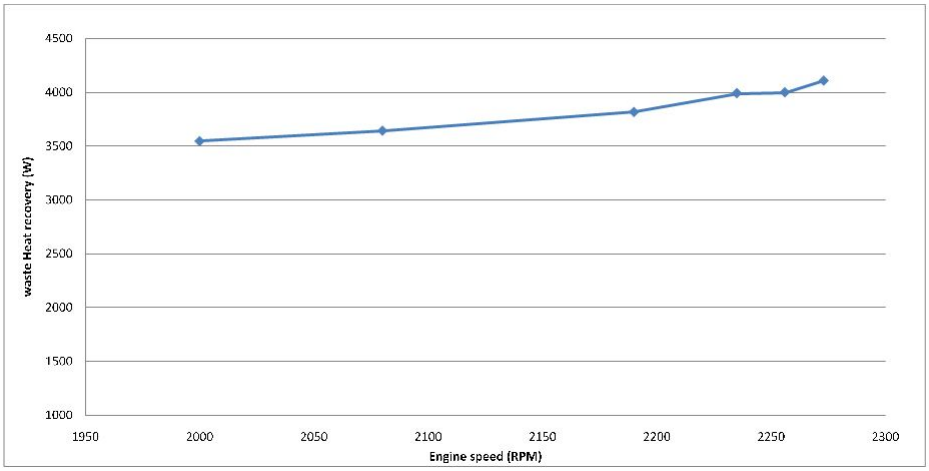

Figure 22: Waste heat recovery from the Diesel engine

To further evaluate the performance of the system, the generator was calibrated to determine its efficiency. Figure 23 shows the power input from a motor to the generator and the output from the generator. The motor power input decreases as the rotational speed increases. On the other hand, the power output of the generator also increases. Hence the efficiency of the generator increases. Figure 24 shows the efficiency of the generator. The average efficiency of the generator is about 50%.

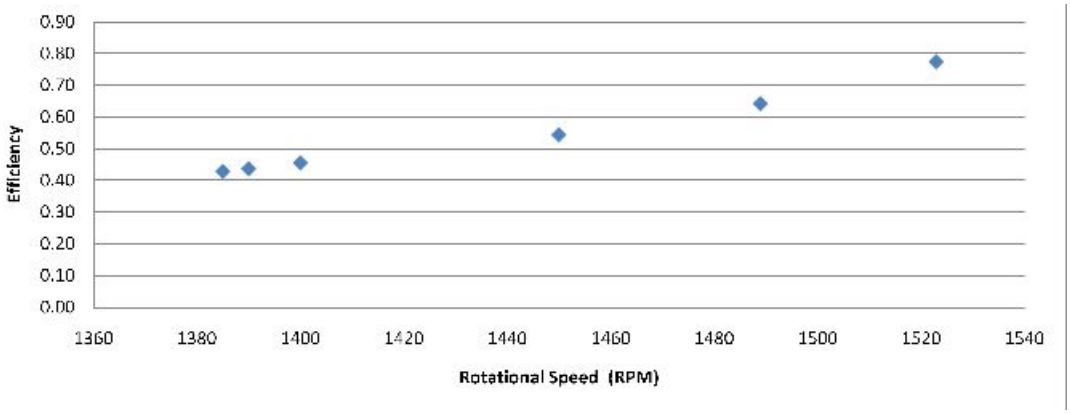

Figure 24: Efficiency of the generator

4.3 Power Output of the System

It was necessary to examine the structure of a steam piston engine in order to better understand the modified Rankine cycle. In the structure of a double-acting steam engine, the volume of each side of the cylinder is different due to the volume of the piston rod as illustrated in Figure 25. Also, when the piston approaches the cylinder head, there is a small clearance volume between the piston and cylinder head. This clearance volume is 2% of the displacement of the steam engine. Based on this clearance, refrigerant could be filled into the clearance, push the piston, and create power. Figure 25 shows the structure of a steam engine.

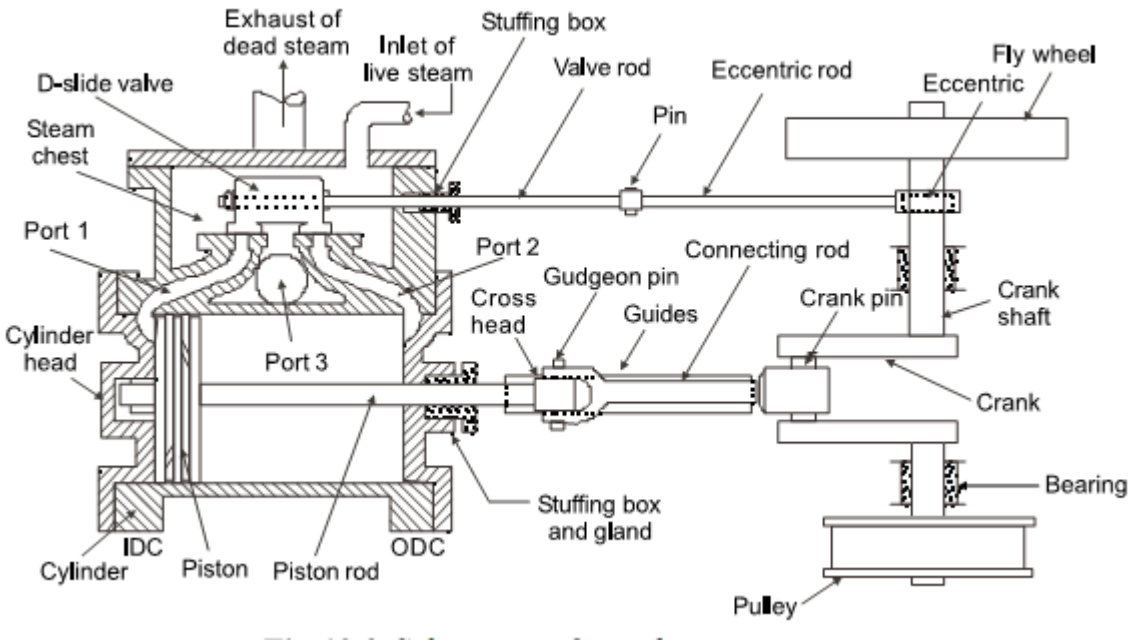

Figure 25: Structure of a double-acting steam piston engine

A P-v diagram of a steam engine cycle helps to evaluate the ideal power output of the steam engine. Figure 26 shows the P-v diagram of a steam piston engine with clearance consideration.

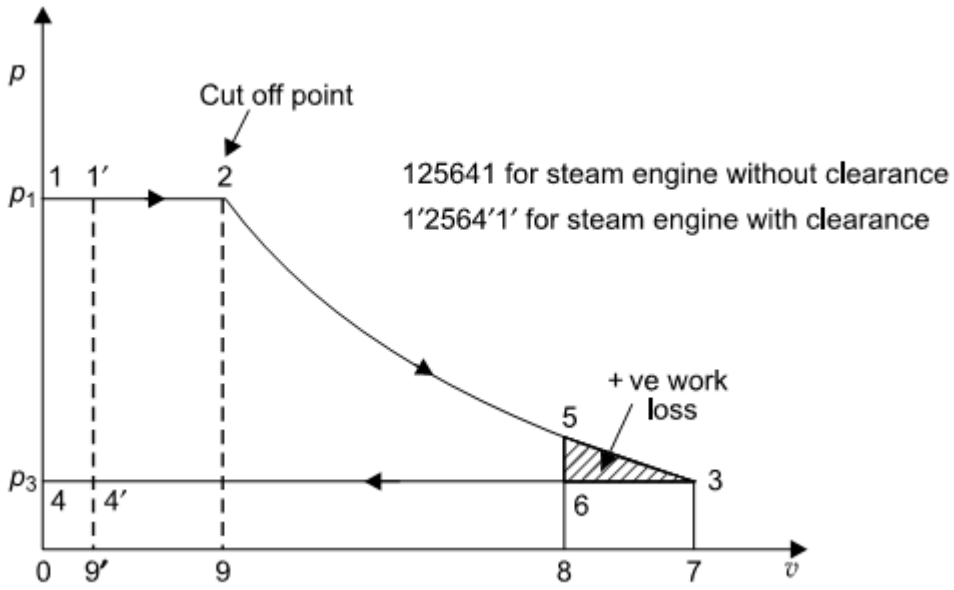

Figure 26: Modified Rankine cycle on a P-v diagram for a steam piston engines

For a steam engine cycle considering the clearance volume, the work would be:

$W = Area\, 1'2564'\, on\, P - v\, diagram$

$W = Area\, 1290 + Area\, 2589 - Area\, 4680 - Area\, 11'4'4$

$W = (P_1V_2) + P_1V_2ln(\frac{V_5}{V_2}) - P_3 \cdot v_6 - (P_1 - P_3)\, V_1'$

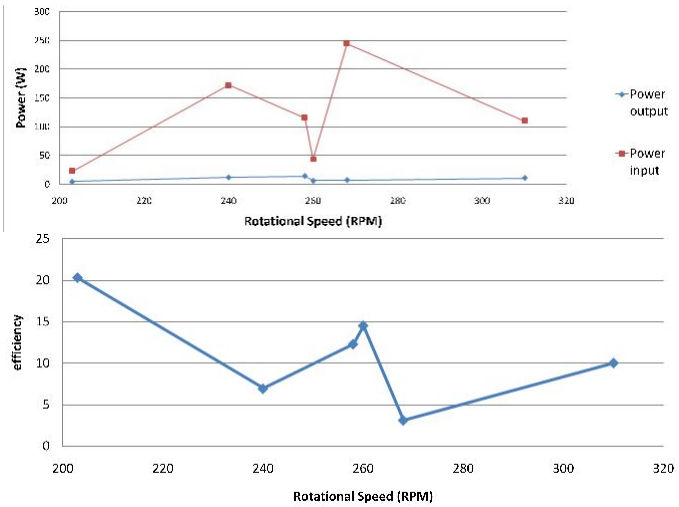

Figure 27: Power and efficiency versus rotational velocity

For the steam piston engine used in the present experiments, the cut-off ratio is 0.55. Therefore, based on the power output of the generator and the rotational speed of the steam engine, one can evaluate the performance and efficiency of the steam engine and the generator combined, as shown in Figure 27 . There was a dip at 260 RPM, due to vapor lock of the pump during the experiment. Vapor lock happens when the refrigerant heats and forms bubbles inside the pump. When I looked through a transparent hose behind the pump, there was not any liquid transport when vapor lock happened; the pump hardly transported any liquid through the heat exchanger. Therefore, there was not enough mass flow rate coming through the steam engine to create enough power output. The maximum power output without vapor lock was 250 Watt at 268 RPM. The vapor lock happened at 260 RPM; hence, the thermal power input plummeted. After I cooled down the pump to avoid vapor lock, the power input to the steam engine was 250 Watts at 268 RPM. The efficiency of the steam engine was highest at 20 % at 203 RPM. However, the power output from the generator was almost constant. Therefore, even though the power input to the steam engine increased, the efficiency decreased.

Further, with knowledge about the pressure and temperature of refrigerant through

the cycle, we could determine the performance of a Rankine cycle. Figure 28 showed the entire Rankine cycle.

State A:

Pressure and temperature at the inlet of the steam engine was $1.3\,MPa$ and 60^oC

The enthalpy of R134a from the heat exchanger was 440 kJ/kg

There was limitation in pressure input to the steam engine. The steam engine pressure limit was $1.3\,MPa$. If the pressure input was higher than the specified pressure, the pin on the fly wheel would have been broken. During the experiment, when the pressure was higher than $1.3\,MPa$, there was some leakage at the connecting rod. Therefore, the limitation of the input pressure restricted the power output of the system.

State B:

Pressure and temperature at the outlet of the steam engine was $0.84\,MPa$ at 45^oC

Enthalpy of R134a exited from the steam engine was 430 kJ/kg

The pressure of the refrigerant was kept at $0.84\,MPa$ in order to transform the refrigerant to liquid at the outlet of the condenser. During the experiment, the room temperature was 30^oC. In order to maintain refrigerant in the liquid phase, the pressure in the low cycle must be at least $0.8\,MPa$.

The specific volume of R134a at state B was $0.0166\,m^3/kg$.

The rotational velocity of the steam engine was 240 RPM. There is a cut-off which is 0.55. Therefore the volumetric flow rate was:

$Q = \frac{RPM*1.98*Displacement*0.55}{60} = \frac{240*1.98*6.5*10^{-5}*0.55}{60} = 0.00028\,(m^3/s)$

The mass flow rate of R134a was: $\dot{m} = \frac{0.00028}{0.0167} = 0.017\,(kg/s)$

Then, the thermodynamic energy input to the steam engine was $q = \Delta h \cdot \dot{m} = (440 - 430) \cdot 0.017 \times 1000 = 170\,(W)$

As one compared the ideal energy output from the steam engine and the change in enthalpy in steam engine, there was a loss of:

$Q_{loss} = q_{Rankine\,output} - q_{ideal\,steam\,engine} = 170 - 150 = 20\,(W)$

This loss was from the hose connecting from the heat exchanger to the steam engine.

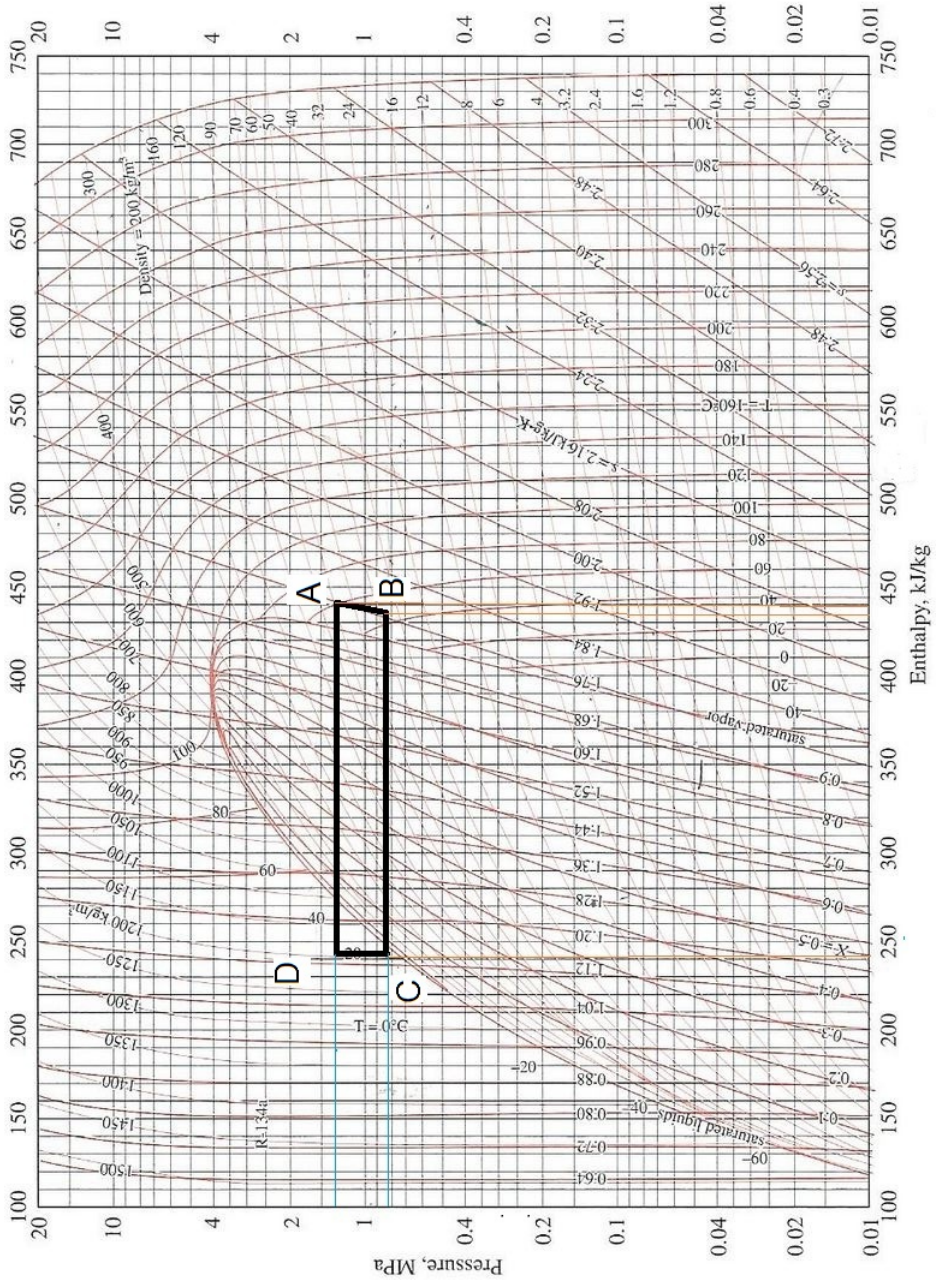

Figure 28: Organic Rankine cycle

State D:

The enthalpy of the refrigerant at the inlet of the heat exchanger was 250 kJ/kg

Hence, the diesel engine provided energy Q_{in} to vaporize the refrigerant from state 4 to state 1 in the Rankine cycle is $q = \Delta h_{HE} \cdot m = (440 - 250) \cdot 0.017 = 3.23\,kW$

The efficiency of the Rankine cycle was:

$$\eta_{Rankine\,cycle} = \frac{\dot{W}_{output}}{\dot{Q}_{in}} = \frac{170}{3230} \times 100\% = 5.2\% \tag{13}$$

At this current setup, the heat transfer from exhaust gas from the Diesel engine is 3.64 kW. Therefore, we can derive the efficiency of the heat exchanger as:

$$\eta_{HE} = \frac{q_{out}}{q_{in}} = \frac{3.23}{3.64} \times 100\% = 89\% \tag{14}$$

At this point, I computed the power output of the combined cycle: the Rankine cycle coupled with the diesel engine output. The power output of the Rankine cycle is much smaller than the power output of the diesel engine. In Figure 28, the curve for the combined cycle is slightly higher than the power output of the diesel engine. Figure 29 shows the power output of the combined Rankine cycle and the diesel engine power.

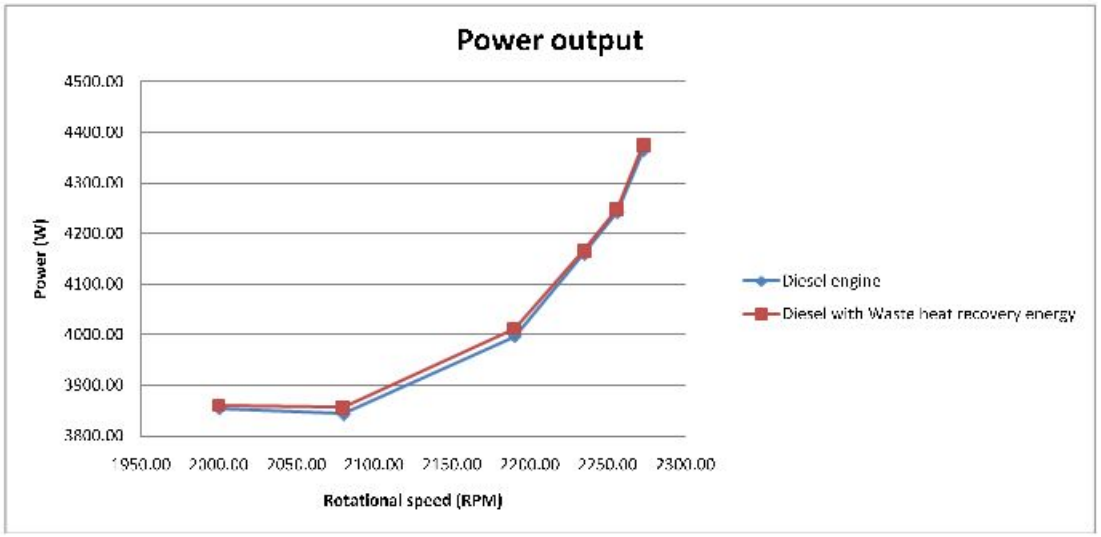

Figure 29: Combined Rankine power output and Diesel engine power output

Another measure to evaluate the performance of the combined Rankine cycle was to evaluate the energy per unit mass of diesel fuel. Figure 30 shows that, as the rotational speed increases, the energy per unit mass increases. This trend is also correlated with Figure 12. In Figure 12, the specific fuel consumption decreases between 2000 RPM to 2500 RPM.

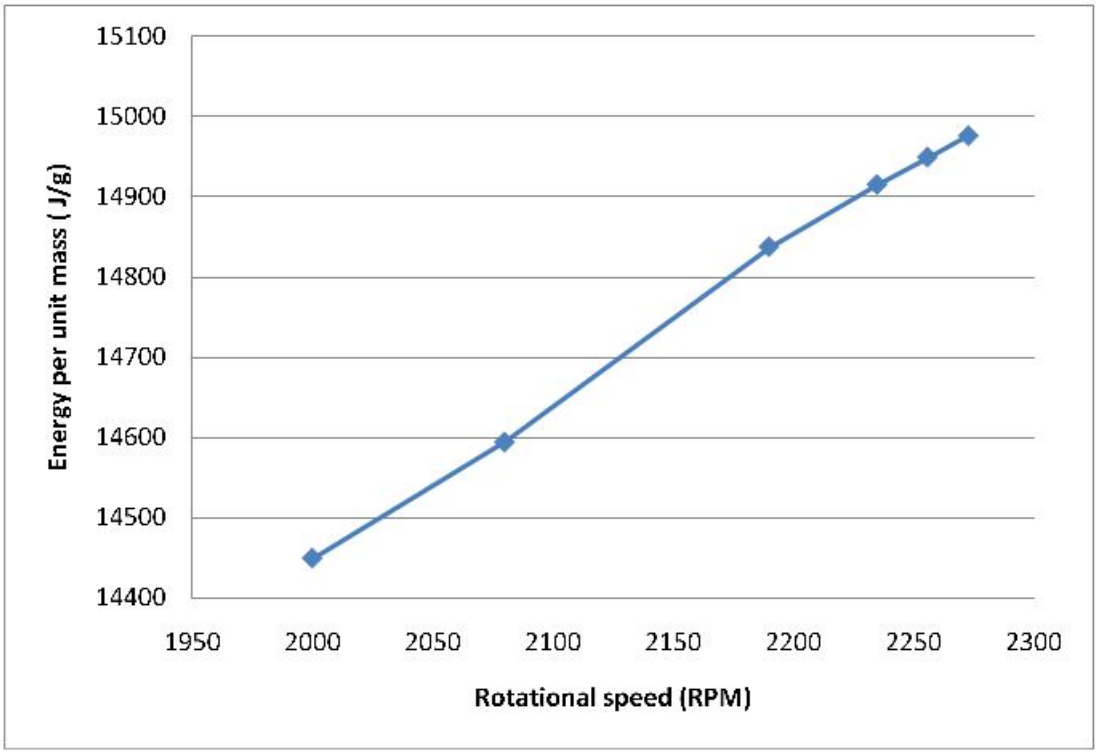

Figure 30: Energy per unit mass of combined Rankine cycle

In order to understand the performance of the organic Rankine cycle, the power outputs of the organic Rankine cycle were scaled with a 6 liter diesel engine displacement. I intended to compensate the frictional loss of vane pumps for a 6 liter diesel engine. The vane pump frictional torques were used as virtual parasitic loss in a 6 liter diesel engine. I need to calculate the brake mean effective pressure (bmep)

$$bmep = \frac{Power}{Swept\,volume\,(m^3) \cdot N\,(RPM)} \tag{15}$$

and we scaled frictional losses to frictional mean effective pressure (fmep):

$$fmep = \frac{2 \cdot \pi \cdot torque}{Swept\,Volume\,(m^3)} \quad (16)$$

Data about the frictional torque of the vane pumps were derived from Inaguma[12]. All of the frictional torques were at a rotational speed of 2000 RPM. Fmep and bmep of the Rankine cycle were scaled by a swept volume of 6 liters from the GMC Sierra 3500. Table 7 shows the fmep of the vane pumps on the diesel engine. Figure 31 shows the fmep of the vane pumps fmep versus different vane widths. In this figure, the fmep increased as the proportional vane pump widths increased. There were three vane widths: 0.9, 1.4, and 1.8 mm.

Table 7: Fmep of vane pump on the 6-liter Diesel engine

vane width (mm)	vane pump frictional torque (N-m)	fmep (kPa)
0.9	0.25	0.26
1.4	0.4	0.42
1.8	0.5	0.52

Table 8 shows bmep of Rankine cycle and the combined cycle:

Table 8: Bmep of Rankine cycle and combined cycle

RPM	Rankine cycle output (W)	Combine cycle output (W)	Bmep of Rankine cycle (kPa)	Bmep of combined cycle (kPa)
2000	4.73	3860	0.023	19.3
2080	11.94	3855	0.06	19.28
2190	14.23	4012	0.071	20.06
2235	6.37	4166	0.031	20.83
2256	7.68	4249	0.038	21.25
2273	11.12	4375	0.056	21.88

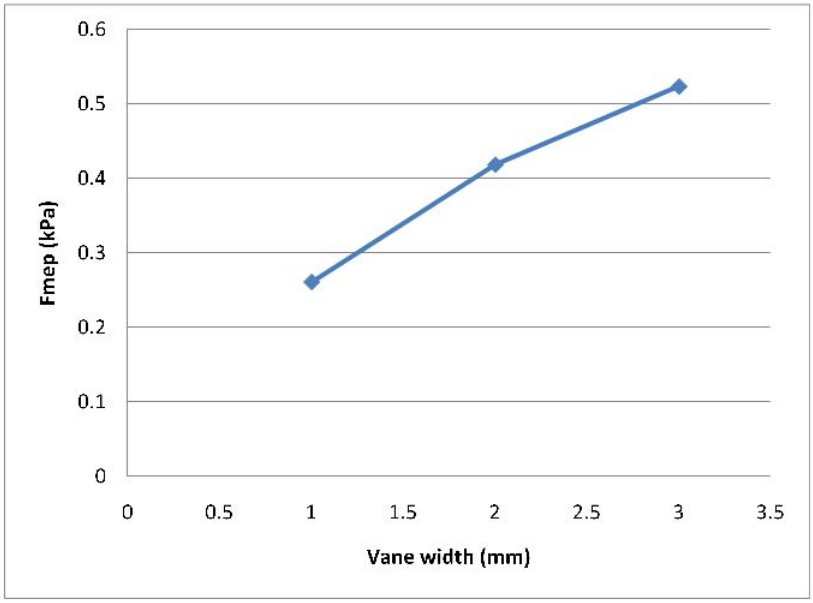

Figure 31: Fmep of vane pump at different vane width

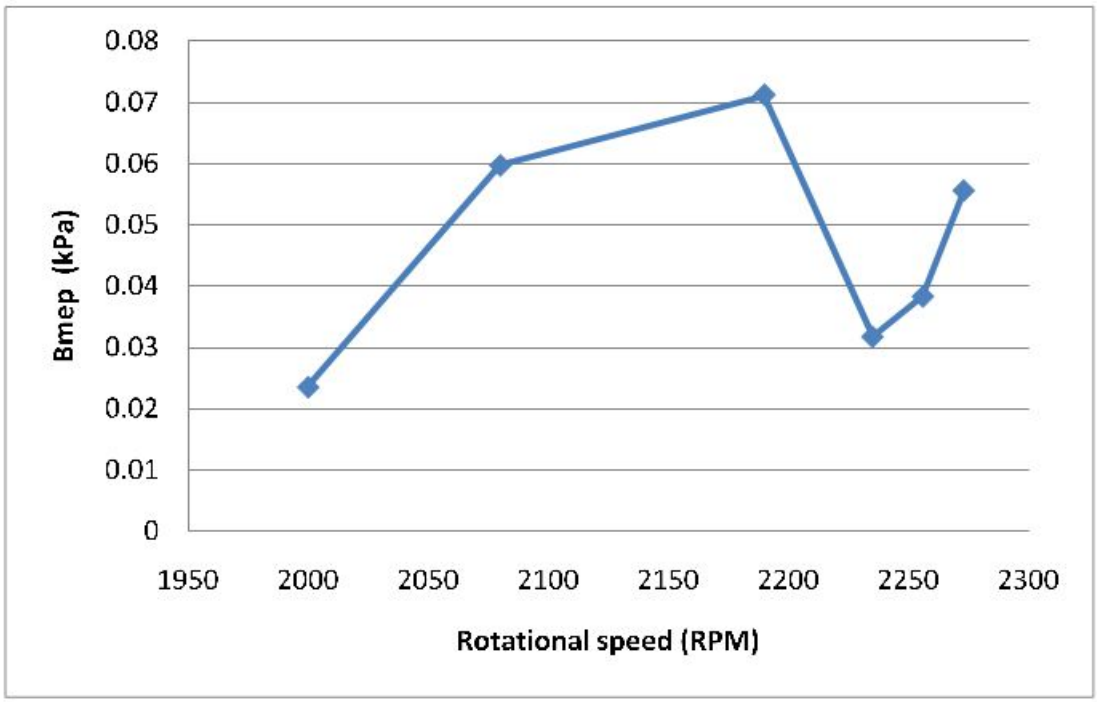

Figure 32: Bmep of Rankine cycle

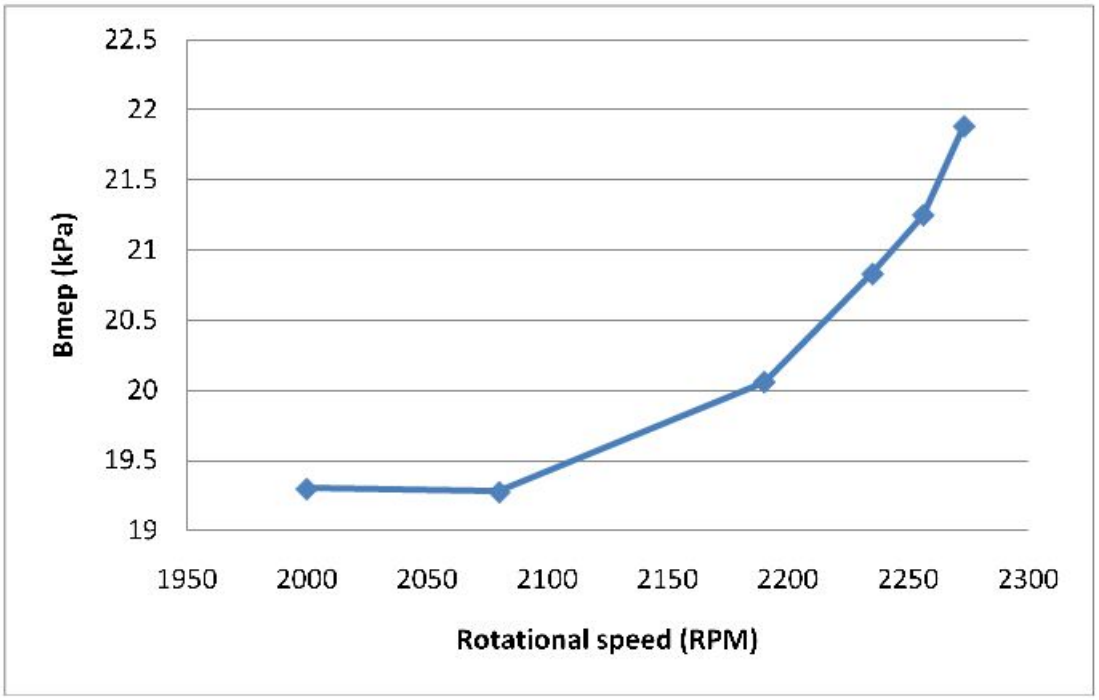

Figure 33: Bmep of combined Rankine cycle

The bmep of Rankine cycle only covered a third of fmep for the vane pump. However, the Rankine cycle contributed in lowering the fuel consumption of the combined cycle.

5 Recommendations and Conclusions

I successfully assembled a combined organic Rankine cycle. The combined organic Rankine cycle extracted energy from the exhaust gas of a diesel engine. I studied significant properties of suitable working fluids. I chose the dry working fluid, R134a, which did not condense when it exited the steam piston engine. R134a is also available in the market while others working fluids require a refrigeration handling certificate. Furthermore, R134a is environmentally friendly with low environmental impact. R134a was compatible with elastomer sealing material. R134a was also compatible with the polyolester lubricant used in our organic Rankine cycle. I also calibrated the components of the combined Rankine cycle. The efficiency of the heat exchanger converting exhaust heat from the diesel engine to vaporize R134a was 89%. The average efficiency of the generator was 50%. The hydraulic pump used for the combined Rankine cycle showed a transporting problem, as vapor-lock occurred when the pump ran for about 1 minute. There were pockets of R134a vapor inside the pump during pumping; and the pump only contracted and expanded the vapor pocket without moving fluid. This problem prevented the operation of the Rankine cycle running continuously. The output of the combined Rankine cycle was normalized to compensate for the parasitic losses of a virtual vane pump used in hydraulic systems for the 6 liter diesel engines. There were three different vane pump widths from different pumps to compare frictional loss. The pump with the smallest vane width presented the least frictional mean effective pressure (0.26 kPa) when scaled with the displacement of the GMC Sierra 6 liter diesel engine. The power output of the Rankine cycle was scaled to brake mean effective pressure to compare with the frictional mean effective pressure. The maximum bmep was at 0.071 kPa when diesel engine had rotational speed at 2190 RPM. The power outputs of the organic Rankine compensated partially the frictional loss of the vane pumps in the 6 liter diesel engine.

The major problem for the low efficiency of 5.2 % was that the upper limit in pressure of the steam engine. The upper pressure limit was only $1.3\,MPa$. I recommended to choose a steam engine which can handle higher pressure. This steam engine needs

harder material for pins and connectors to sustain higher pressure. Another problem with R134a was that it needed to be kept at high pressure at $0.8\,MPa$ to keep in liquid state at room temperature 30^oC; hence, the small difference in pressure lead to low power output in the organic Rankine cycle. Due to the condensing pressure similarity to R134a, R1234yf cannot be used to improve the efficiency of the organic Rankine. The P-h diagram of R1234yf was presented in the Appendix A. Thus, different refrigerants having lower vaporization pressure at room temperature (30^oC) are needed in order to improve the efficiency of the combined organic Rankine cycle. Potential refrigerants are R123 ($0.1\,MPa$), R114 ($0.25\,MPa$), R21 ($0.2\,MPa$). Further, in this research project, the pump showed vapor lock problem. There was a need to replace this pump with refrigerant compatible pumps. At Klausunion, there is Sealess Multi-stage Regenerative Turbine Magnetic Drive Pump which is compatible with refrigerants and increases pressure up to $580\,psig$. Besides replacing the pump, it is also helpful to cool down refrigerant in the condenser. Therefore, one can increase the capacity of the condenser to avoid transporting problem in the pump.

A Appendix A: Refrigerant Mollier Charts

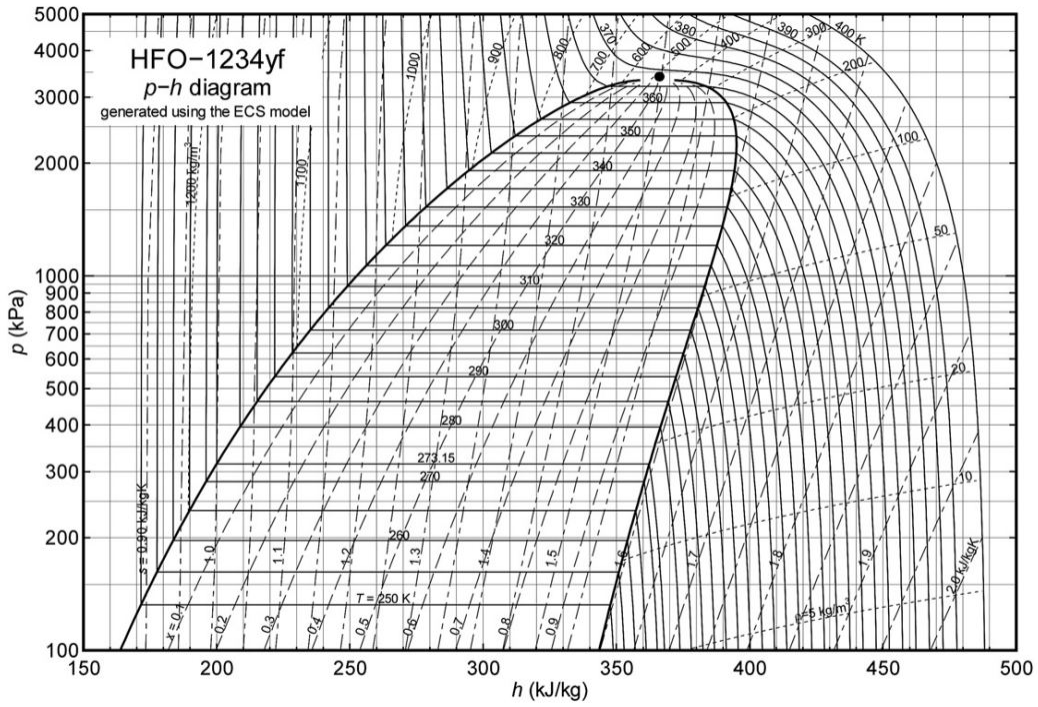

Figure 34: Mollier Chart of R1234yf. Courtesy of Akasaka[3]

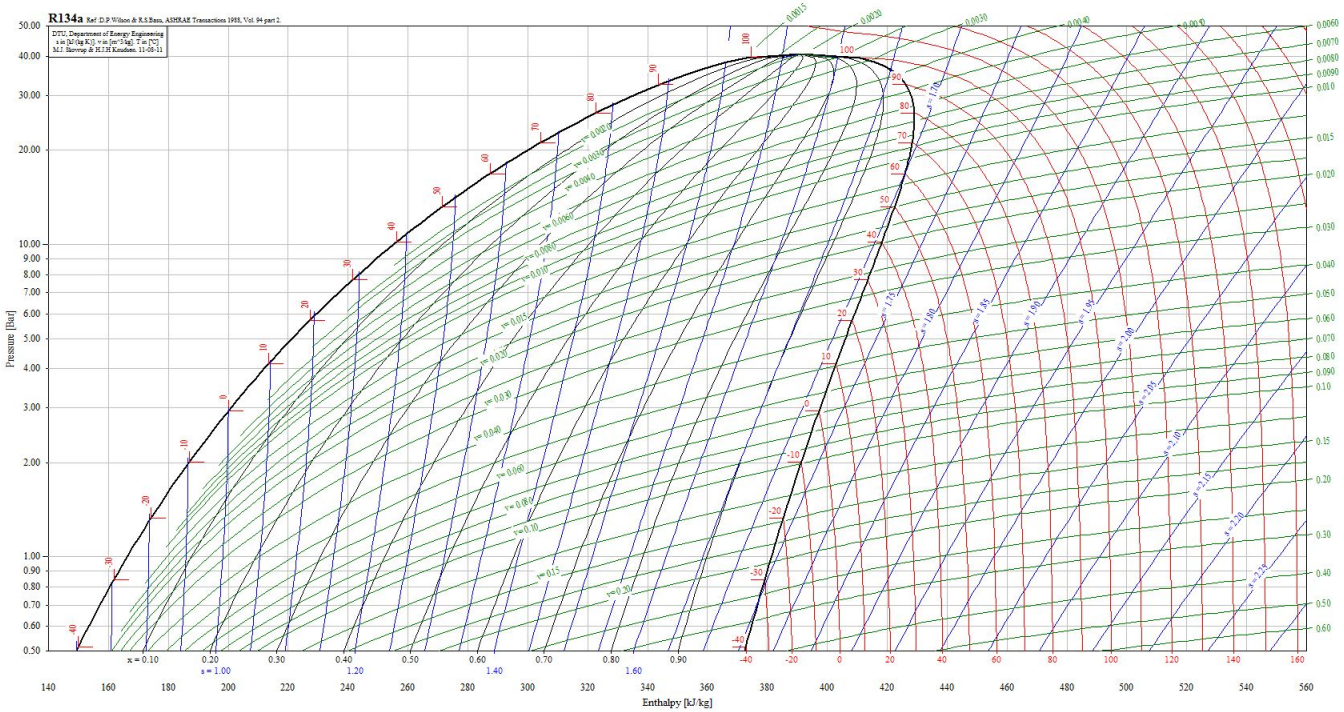

Figure 35: Mollier chart of R134a. Courtesy of CoolPack

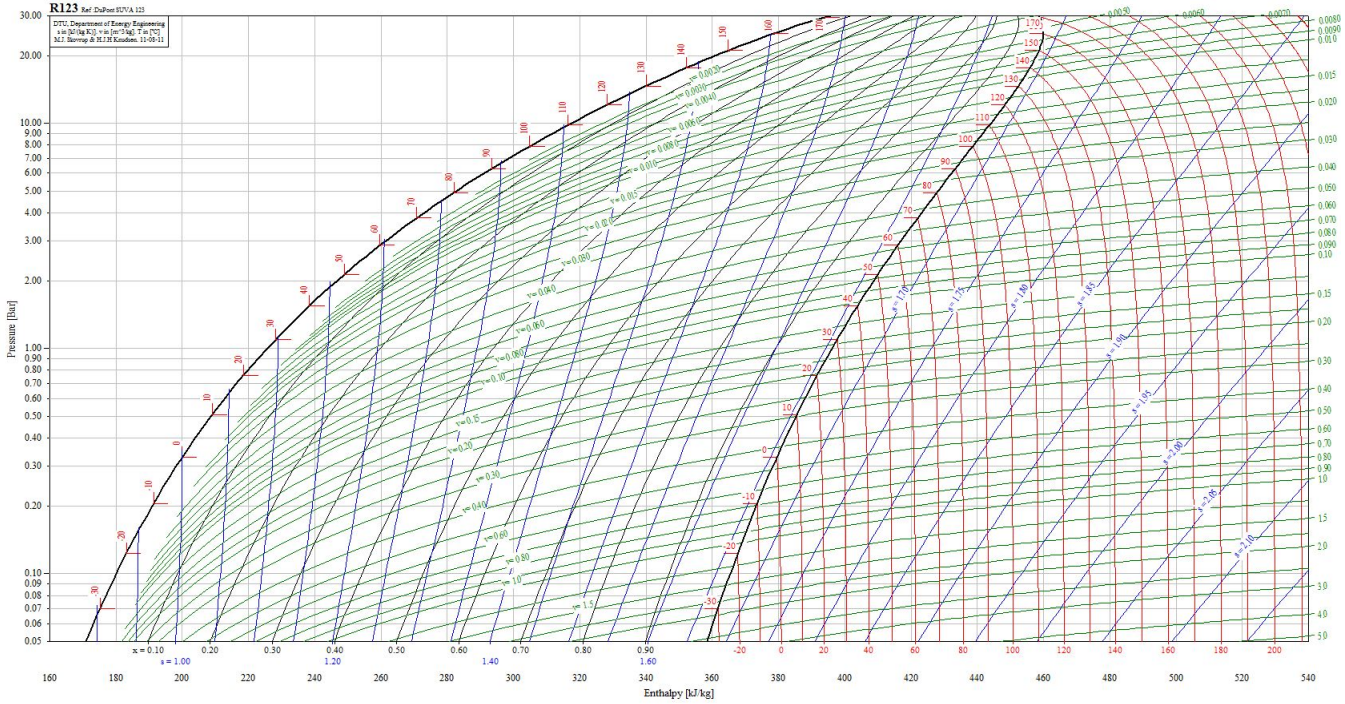

Figure 36: Mollier chart of R123. Courtesy of CoolPack

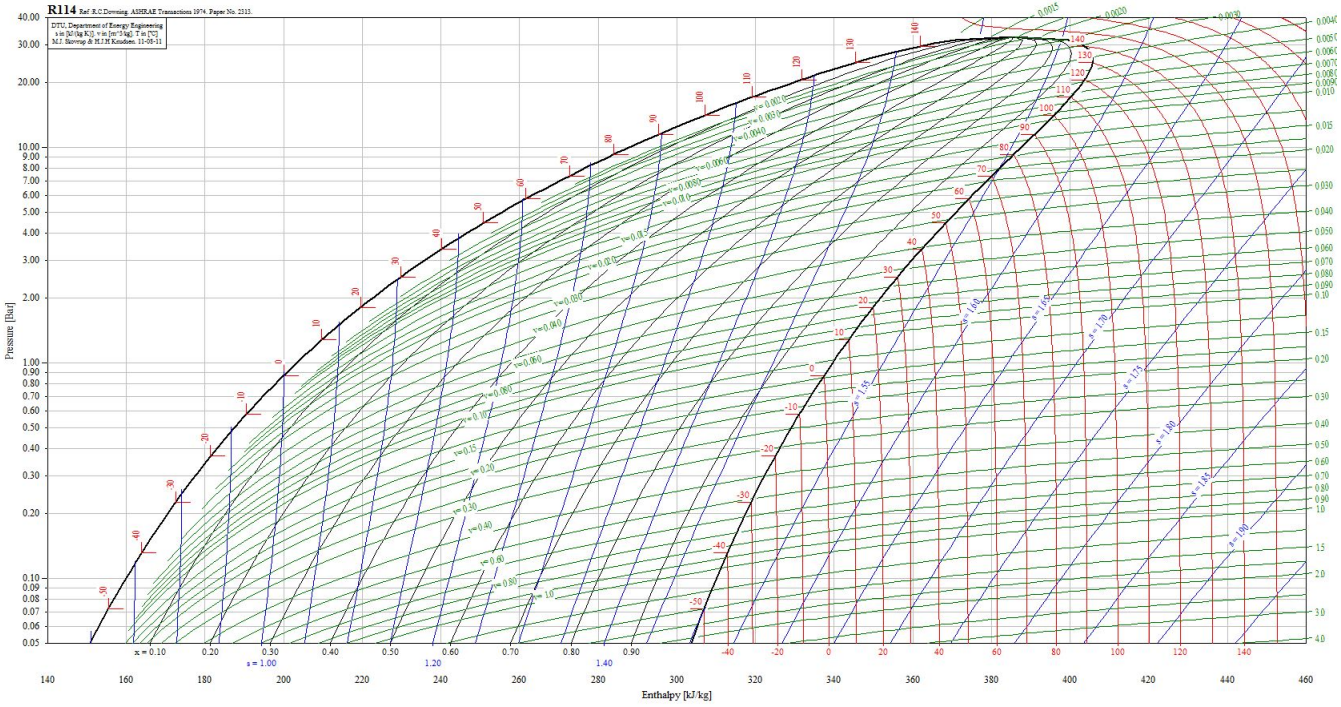

Figure 37: Mollier chart of R114. Courtesy of CoolPack

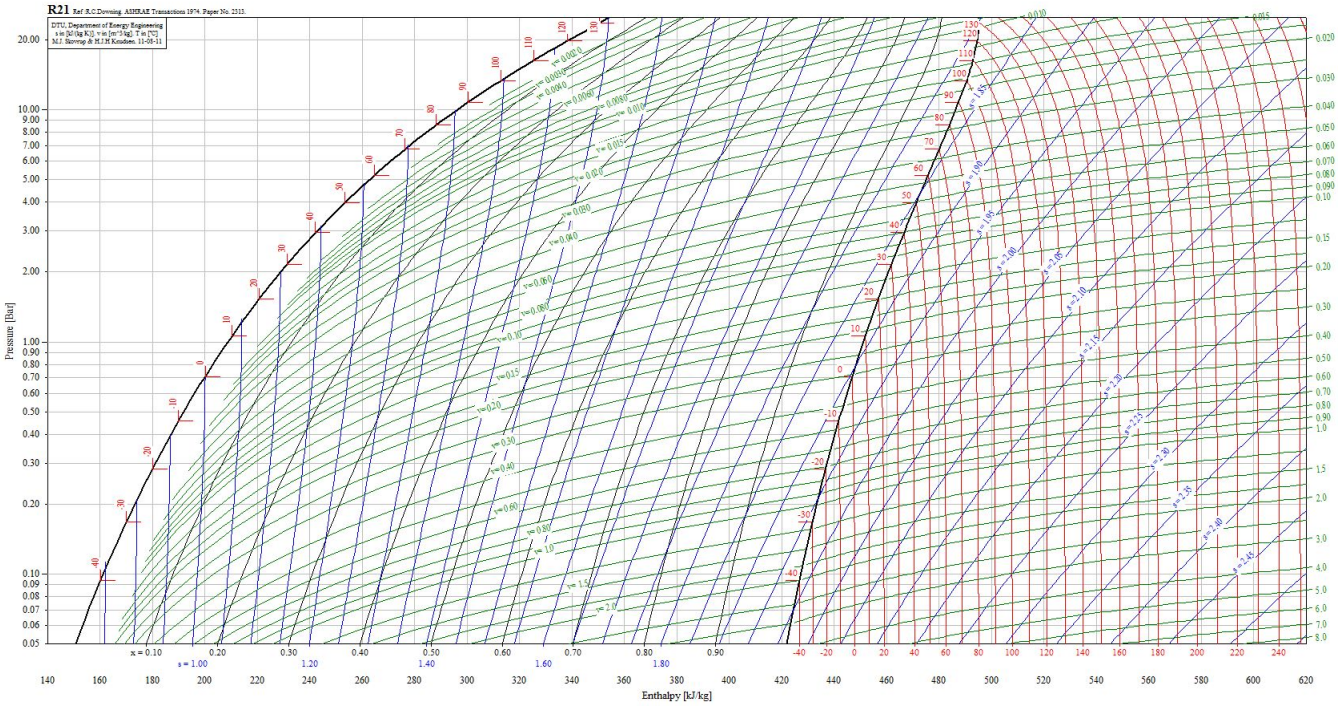

Figure 38: Mollier chart of R21. Courtesy of CoolPack

B Appendix B: Calibration Result

The linear curve, $y = -0.0118 \times x + 2.131$, was used to calculate the mechanical power output of the motor used to calibrate the generator.

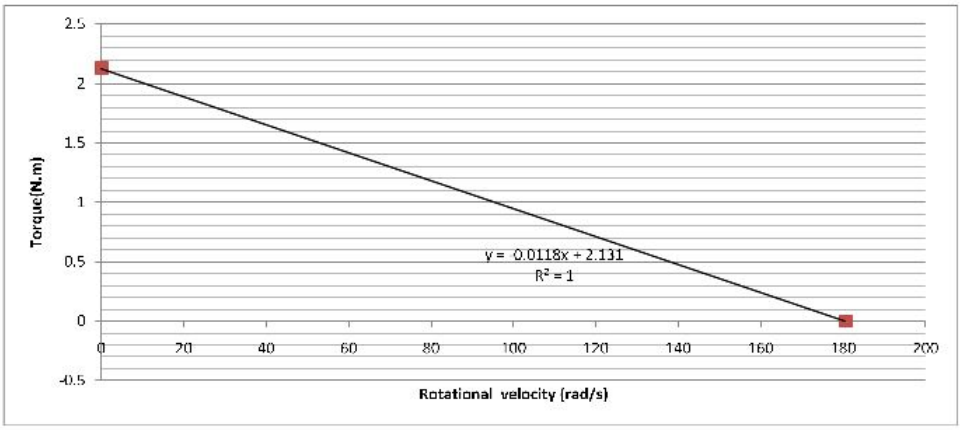

Figure 39: Torque versus rotational speed of motor

C Appendix C: Instruction to use CoolPack

CoolPack is a software package which provide thermodynamic properties of refrigerants. CoolPack was developed by the Department of Mechanical Engineering at Technical University of Denmark in 2000. Their website is: www.et.dtu.dk/CoolPack.

Start CoolPack from *Start* menu.

Choose $Refrigerant Utilities$ from the Toolbar. In Figure 40, the $Refrigerant Utilities$ button was in the circle.

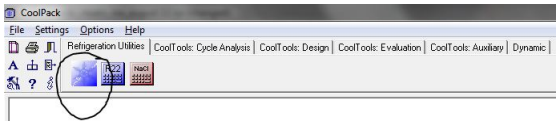

Figure 40: CoolPack toolbar

Then, the $Refrigerant Utilities$ window shows up like in Figure 41.

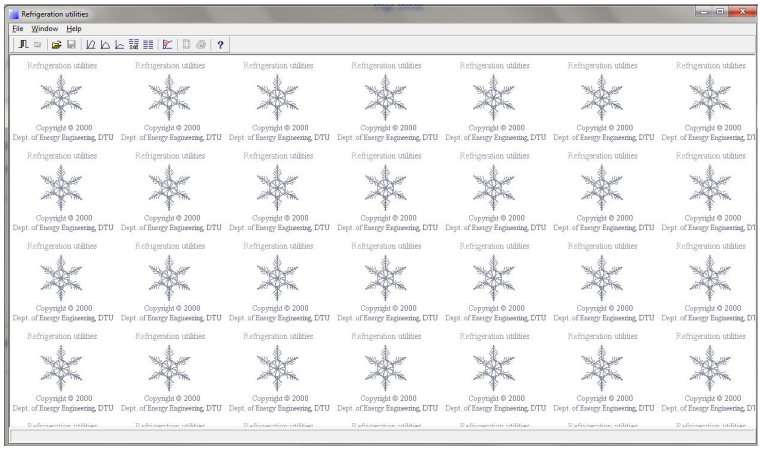

Figure 41: Refrigerant Utilities window

Then press Shift+Ctrl+L to open $Set properties for log(P) - h diagram$.

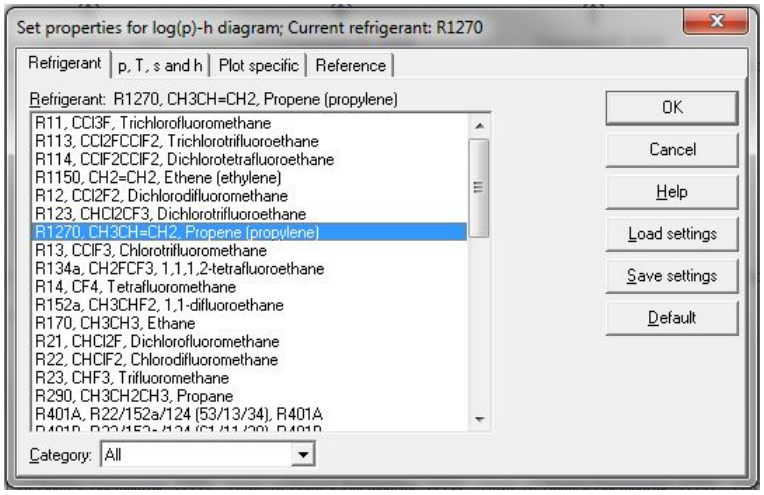

Figure 42: Set properties for log(P)-h diagram

References

[1] Yanmar l100ae diesel engine.

[2] *2001 Ashrae handbook Fundamentals*. American Society of Heating, Refrigerating and AIr-Conditioning Engineers, Inc., si edition, 2001.

[3] Ryo Akasaka, Katsuyuki Tanaka, and Yukihiro Higashi. Thermodynamic property modeling for 2,3,3,3-tetrafluoropropene (hfo-1234yf). *International Journal of Refrigeration*, 33:52–60, 2010.

[4] Marco Badami and M. Mura. Preliminary design and controlling strategies of a small-scale wood waste rankine cycle(rc) with a reciprocating steam engine(se). *Energy*, 34:1315–1324, 2009.

[5] Mike Brown. *The Mike Brown Steam Engine with The Basics of Steam Engine*. Springfield, Missouri, third edition, 1997.

[6] Yunus A. Cengel and Michael A. Boles. *Thermodynamics An Engineering Approach*. Mc Graw Hill, sixth edition, 2008.

[7] Y. Chen, P. Lundqvist, A. Johansson, and P. Platell. A comparative study of the carbon dioxide transcritical power cycle compared with an organic rankine cycle with r123 as working fluid in waste heat recovery. *Applied Thermal Engineering*, 26:2142–2147, 2006.

[8] Robert G. Doerr, Scott T. Jolley, and Raymond H.P. Thomas. *1998 ASHRAE HANDBOOK REFRIGERATION SI Edition*. ASHRAE, 1998.

[9] Glenn Elert. Energy density of diesel fuel. The Physics Factbook.

[10] R.C. Gunderson and A. W. Hart. *Synthetic Lubricants*. Reinhold Publishing Corporation, NY, 1962.

[11] G.R. Hamed and R.H. Seiple. Compatibility of refrigerants and lubricants with elastomers. Technical report, Air-Conditioning and Refrigeration technology Institute, Arlington, VA, 1993.

[12] Y Inaguma and A Hibi. Vane pump theory for mechanical efficiency. *Journal of Mechanical Engineering Sciency*, 219, 2005.

[13] Maria Jonsson and Jinyue Yan. Ammonia–water bottoming cycles: a comparison between gas engines and gas diesel engines as prime movers. *Energy*, 26:31–44, 2001.

[14] Vimal Kumar, Supreet Saini, Manish Sharma, and K.D.P. Nigam. Pressure drop and heat transfer study in tube-in-tube helical heat exchanger. *Chemical Engineering Science*, 61:4403–4416, April 2006.

[15] Thomas J. Leck. Evauation of hfo-1234yf as a potential replacement for r-134a in refrigeration application. *3rd IIR Conference on Thermophysical Properties and Transfer Processes in Refrigerants,Boulder, CO, 2009*, 2009.

[16] Vincent Lemort, Cristian Cuevas, Jean Lebrun, Ion Vladut Teodore, and Sylvain Quoilin. Development and experimental validation of an organic rankine cycle model. *Heat SET*, April 2007.

[17] MicroMo. Motor calculations.

[18] Onkar Singh. *Applied Thermodynamics*. New Age International Publishers, third edition, 2009.

Vita

Tai Anh Duong was born in Vinh Long, Vietnam on the 2nd of January, 1987, the son of Mai Huong Nguyen and Nam Duong. After completing his Bachelor of Science degree in Mechanical Engineering from New Jersey Institute of Technology, Newark, New Jersey, in 2009, he entered the Graduate School at the University of Texas at Austin to further his study in Mechanical Engineering with a focus on Thermal Fluid Systems in the fall of 2009. He completed his Master of Science degree in Mechanical Engineering in August 2011.

Permanent Address: B21 Nam Thong 1, District 7,

Hochiminh city, Vietnam 00848

This thesis was typed in Lyx by the author.